UNIVERSITÀ DEGLI STUDI DI TORINO

Ph.D. Programme in Complex
Systems for Life Sciences

XXXIII cycle

Purinergic Signaling in Tumor Vascularization

Giorgia Scarpellino

Tutor: Prof. Luca Maria Munaron

Contents

Abstract

Tumor microenvironment (TME) alterations are active players during multiple stages of cancer progression, including tumor vascularization[1]. Accumulation of extracellular ATP (eATP) is considered as one of TME hallmarks[2,3] and leads the continuous purinergic receptors (PRs) stimulation both in cancer and stromal cells, the latter including endothelial cells (ECs).

PRs family is divided into two sub-families: the metabotropic P2Y receptors (P2YRs) and the ionotropic P2X receptors (P2XRs)[4]. They represent an interesting subject of study since their known sensibility to several TME hallmarks including acidosis[5–8], hypoxia[9,10] and increased extracellular matrix (ECM) stiffness[11,12]. Today, growing consensus regards eATP and other nucleotides as central players in cancer and immune cells proliferation and migration[13] , but the direct role of purinergic signaling in tumor vascularization is still controversial.

The focus of my Ph.D. has been to investigate the effects of PRs activation in breast cancer-derived ECs (BTECs). Starting from the evidence that high eATP concentration (> 20 μM) exerts a strong anti-migratory activity in BTECs[14], we studied the Ca^{2+} Signaling toolkit activated by high ATP stimulation (100 μM) and its correlation with

the inhibitory effect on BTECs migration. Then, we deeper investigated the functional role of P2X7 ionotropic receptor (P2X7R) activation, often overexpressed in cancer cells, by using the ATP analog BzATP. Stimulation with BzATP mimics the effect of ATP, by inhibiting only BTECs and not normal ECs (HMECs) migration. The effect of P2X7R activation was evaluated in BTECs, HMECs, in ECs derived from renal and prostate cancers (respectively RTECs and PTECs) and in HMEC co-coltured for 72h with a human breast cancer cell line (MCF-7).

In conclusion, data presented in this thesis indicate that high purinergic stimulation activates a TEC-specific pathway that inhibits cells migration passing through the activation of P2X7R. No correlation was found between the Ca^{2+} signals elicited following the receptor activation and the functional effect but interestingly, the extracellular environment conditions alter the activation of the intracellular pathway responsible for the anti-migratory effect.

Introduction

1. Tumor Microenvironment

In addition to cancer cells, tumors include different components continuously interact with each other. The interaction between cancer cells and the surrounded elements creates the tumor microenvironment (TME): a complex and dynamic network that strongly impacts on tumor development[15]. Cancer cells, in fact, are skilled in recruit supporting cells from nearby endogenous tissue stroma to promote critical early steps of tumor progression. The structure and composition of TME vary between cancer types and patients[16], as well as the genotypes and phenotypes of cancer cells. In order to suggest a conceptual rationale for this diversity, six hallmarks of cancers have been defined: sustained proliferative signaling, escape from growth suppressors, replicative immortality, resistance to cell death, capability for invasion and metastasis, and induction of angiogenesis[17].

In general, is possible to divide between cellular and non-cellular components of TME. Besides cancer cells there are, in fact, the tumor stroma cells, including the immune infiltrate[18], fibroblasts[19] and a complex and disorganized vasculature (both blood and lymphatic vessels)[20,21]. On the other hand, the extracellular matrix (ECM) surrounding

tumors and the biochemical/biophysical stimuli it generates, represents the non-cellular component of TME[15,22].

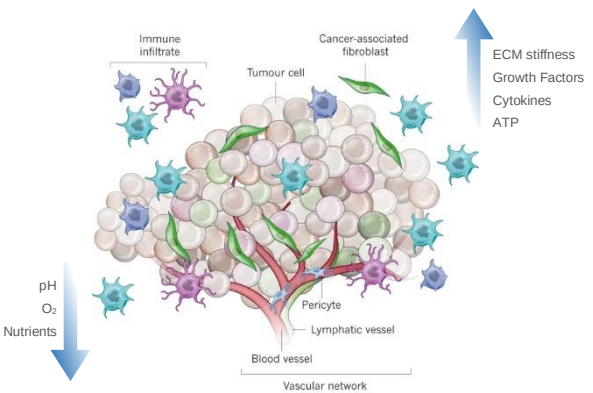

Figure 1. Schematic representation of TME. Tumor cells together with the vascular network, immune infiltrate and cancer-associated fibroblasts, constitute the cellular component of TME. Stimuli from the extracellular environment (matrix stiffness, growth factors and cytokines, ATP accumulation) constitute the non-cellular component of TME.
Image modified from Junttila and de Sauvage, Nature, 2013.

1.1 The Cellular Component of TME

Cancer cells trigger the onset of the disease, carrying oncogenic and tumor suppressor mutations. Among them, a subpopulation of cells is represented by cancer stem cells (CSCs)[23], one of the main challenges of conventional chemotherapy, with their capabilities of self-renewal and multi-lineage differentiation that drive tumor growth and heterogeneity[18]. CSCs originate throughout cancer progression and can further be induced from differentiated cancer cells via the adaptation and cross-talks with the TME[23].

There is a powerful link between inflammation and tumor development[24]. The inflammatory and immune cells, with the myriad of mediators released by them, influence tumor growth by regulating processes such as migration and differentiation of all cell types within TME, including neoplastic cells, fibroblasts and endothelial cells (ECs)[24]. In TME, as a result of inflammation, there are both adaptive (T and B lymphocytes) and innate immune cells (leukocytes such as neutrophils, dendritic cells, macrophages, etc.)[25]. Interesting, cancer cells themselves produce cytokines and other mediators attracting immune cells, that in turn release an assorted array of cytokines, cytotoxic mediators (i.e. reactive oxygen species - ROS), proteases, interleukins and interferons (IFNs) and can either

suppress or promote tumor growth[26,27]. In this context, macrophages are the most prominent components of the innate immune system in cancer[28]: they mainly orchestrate cancer-related inflammation by playing a dual role (pro- or anti-tumor activity) depending on their state[27]. Although they may present tumor antigens to T cells, which are then activated to kill tumor cells, they also may promote the escape of tumor cells into the circulatory system and suppress the anti-tumor immune response. In this light, many studies revealed the presence of tumor-associated macrophages (TAMs) that usually accelerate vessel growth, thus promoting tumor survival, through the up-regulation and release of several pro-angiogenic factors[26,28,29]. Interestingly, TME itself polarizes macrophages toward tumor-support M2 or a mixed M1/M2 phenotype, which serves as a major source of pro-angiogenic factors, boosting the angiogenic switch[28].

Even if stroma composition varies significantly between tumors, fibroblasts usually represent one of the most abundant cell component[30]. In normal tissue, fibroblasts produce and organize various ECM proteins, essential for tissue homeostasis. They also contribute to the production of attractive mediators for immune cells and, depending on the stimuli received, fibroblasts can initiate responses to synthesize and/or degrade particular ECM

structure and molecules[30]. During cancers, fibroblasts switch from physiological and quiescent fibroblasts to activated cancer-associated fibroblasts (CAFs)[31] that display inexhaustible protein synthesis and contractile functions, excessive secretory and ECM remodeling phenotypes, thus actively promoting cancer cell invasion and metastasis[30]. Moreover, CAFs can be diverse in origin, arising from adipocytes, stellate cells, bone-marrow-derived mesenchymal cells, pericytes and ECs[32].

Blood vessels are key components of TME, they ensure the supply of oxygen (O_2) and nutrients, deliver immune cells and hamper the accumulation of metabolic waste, guaranteeing tumor growth[33]. All components of TME, in fact, activate to produce pro-angiogenic factors and promote the angiogenic switch, of which ECs are the main actors. ECs define the inner and thin monolayer of blood vessels that regulates exchanges between the bloodstream and the surrounding tissues[33]. In general, during the early stages of tumor development, cancer cells rely on passive efflux for gas exchange and nutrients transport and only once tumor reaches much volume (1-2 mm^3), it becomes hypoxic and acidic because of the insufficient O_2 and accumulation of metabolic waste[33]. The hypoxic TME leads to the activation of Hypoxia-Inducible Factors (HIFs), the transcription factors

master regulators of Vascular Endothelial Growth Factor (VEGF) expression, that initiate vessels sprouting by instructing ECs to secrete different pro-angiogenic factors (VEGF as well as Platelet-Derived Growth Factor and Epidermal Growth Factor, respectively PDGF and EGF) acting by paracrine and/or autocrine manners[34]. This imbalance between pro- and anti-angiogenic factors, with the predominance of angiogenic stimulators, induces ECs to form new blood vessels lumens, leading the angiogenic switch. In physiological conditions, pericytes are positioned around EC junctions to confer vessel stability and form an umbrella-like structure that covers gaps between ECs, regulating barrier function[21]. Conversely, in tumor vessels, pericytes are not associated with ECs, permitting cancer cells intravasation into the circulatory system and metastasization[35].

1.1.1 Tumor Endothelial Cells

As described in the previous paragraph, tumors develop their own vasculature to overcome the hostile conditions of TME, by orchestrating ECs responses. Agents like hypoxia and chronic growth factor stimulation, lead to a dysfunctional tumor endothelium that differs from that in normal blood vessels. Tumor ECs (TECs) compared to Normal

ECs (NECs) are functionally, morphologically and cytogenetically different[36]. At functional level, TECs are resistant to apoptosis and do not undergo senescence *in vitro*, showing a constant ability to grow and organize persistent capillary-like structures in the absence of serum[37]. Morphologically, they distinguish from NECs because of their irregular shape and size, ruffled margins and long and fragile cytoplasmic projections which extend outward the vessel lumen[36]. Moreover, TECs are aneuploid and display aberrant multiple centrosomes, on the contrary, NECs are diploid with normal centrosomes and remain stable in culture[38]. Several studies show TECs to express unique markers that distinguish them from their normal counterparts and express several genes of yet unknown function, such as receptors for adhesion to the matrix and to circulating leukocytes, and receptors for angiogenic growth factors absent or barely detectable in established blood vessels[39]. Nowadays we are aware of the diversity between TECs and NECs, but previously TECs were considered genetically stable compared with tumor cells and therefore used as an ideal therapeutic target in the development of antiangiogenic treatments.

The morphological abnormalities in tumor vasculature actively contribute to cancer progression, e.g. favoring metastasis spreading, and

considering that vasculature is the main supply line and removal conduit for waste products in tumors, hypoxia and hypoperfusion are natural consequences of impaired blood flow and, at the same time, the major contributors to the hostile conditions of TME[40]. Tumor vessel abnormalities develop as consequence of different factors, one of which is the biochemical tension exerted by tumor mass on surrounding blood vessels, thus resulting squeezed and compressed[41]. Moreover, chronic growth factors stimulation promotes sprouting and excessive branching of endothelial tip cells leading to an irregular monolayer of TECs with the loss of barrier function[36]; the tips of some branched TECs may penetrate lumen and create openings or small intercellular gaps in the vessel wall. These openings allow extravasated erythrocytes to pool at the periphery of tumor blood vessels forming "blood lakes" which are not anastomosed with the vasculature[36]. The appearance of tumor endothelium is described as "mosaic" because of spotty immunoreactivity *in vivo* of the endothelial marker CD31/PECAM-1 (Platelet Endothelial Cell Adhesion Molecule-1)[42]. This chaotic pattern of blood flow and tumor vessel instability may be exacerbate by the aberrant expression of flow-mediated transcription factors and by the fails in reaching the final stage of vessel maturation, represented by pericytes coverage[43]. Thus, leaky

vasculature missing in proper cell-to-cell interaction enables cancer cells to escape the primary tumor site and enter the vasculature (intravasation). During intravasation, tumor cells adhere to ECs and this interaction further changes the endothelial barrier, allowing tumor cells to migrate between two ECs[33]. Tumor cells expressing VE-cadherin may fill in these gaps and masquerade as endothelium[44], even if this topic remains controversial[45].

Despite differences, tumors may recruit vasculature by the same signals elaborated during other physiological or pathological processes. In support of this hypothesis, some endothelial markers were found to be expressed in tumor-associated as well as in normal vessels associated with wound healing, suggesting the idea that tumors are "wounds that never heal" [46].

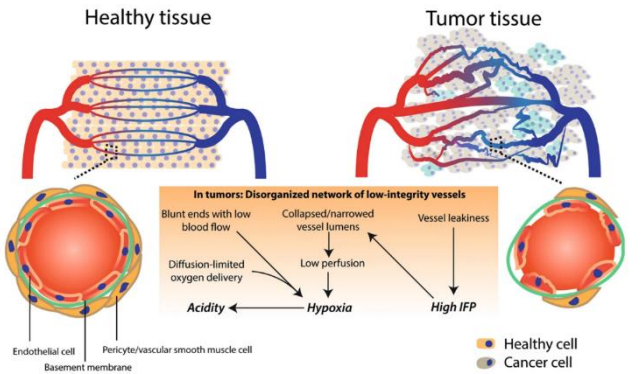

Figure 2. Schematic representation of the vascular network in healthy and tumor tissue. In healthy tissues, a well-organized vessel network ensures full-covering of nutrient supply. These vessels are matured with an endothelial cell layer surrounded by a basement membrane and pericytes. Oppositely, in tumor tissues the vascular network is chaotic, low in pericyte coverage and has loose inter-endothelial cell junctions.
Schaaf et al., Cell Death & Disease, 2018.

1.1.2 Tumor Vascularization

New blood vessel production is a complex and dynamic process that involves and coordinates different cellular types and metabolic ways[47]. In addition to embryonic and fetal development, it may occur during adult life in both health and

disease[48]. Stimulation of angiogenesis may be therapeutic for example in ischemic heart disease and wound healing but on the contrary, in cancer many therapeutic efforts focus on inhibit the angiogenic process with the purpose to hamper cancer growth and metastasis[48]. Currently, anti-angiogenic therapies using either antibodies[49] or tyrosine kinase inhibitors[50] have been approved to treat several types of cancer. One of the compounds commonly used is bevacizumab, an antibody targeted against the VEGF which increases survival in colorectal cancer patients[48]. Other drugs inhibit important kinases for pro-angiogenic stimuli (e.g., sorafenib and sunitinib), or molecules that can block calcium channels (e.g., Carboxyamidotriazole – CAI) or calcium signals which are important in tumor angiogenesis[1,51]. Nevertheless, is well established that the response to vascular targeting therapy is limited, due to a resistance acquired from the majority of patients. This partial failure may be due to different factors including the previously described high instability of ECs within tumors[52], the continuous recruitment of circulating Endothelial Progenitor Cells (EPCs), that results insensitive to VEGF stimulation[53], the capability of TECs to acquire resistance to drugs and also, the ability of tumors to find alternative ways for their sustenance.

There are two main mechanisms by which new blood vessels originate, and both of them take place during cancer: vasculogenesis and angiogenesis[53]. Vasculogenesis represents the *de novo* formation of a primitive vascular network and is defined by the differentiation of EPCs, or angioblast, into ECs[54]. However, this process is not limited to the embryo life, it may occur as a para-physiologic mechanism and verify when, in response to different stimuli, EPCs mobilized from bone marrow to the site of new vascularization[54]. This "homing" of circulating EPCs is an essential step in re-vascularization following acute vascular injury but, conversely, in cancer represent one of the main causes of tumor regrow following irradiation[53,54]. Angiogenesis is the process responsible for the remodeling and expansion of vascular networks. It refers to the formation of new blood vessels from the pre-existing ones and typically regards the growth of new capillaries, which are distinguished from vessels by the lack of a fully tunica media development[55]. Angiogenesis may occur either via sprouting or intussusception, both during pre-natal and adult life. The sprouting process is based on ECs migration, proliferation and tube formation, accompanied by dissolution of ECM and completed by the intervention of pericytes to confer vessel stability[56]. Intussusception divides existing vessel lumens by formation and insertion

of tissue folds and columns of interstitial tissue into the vessel lumen; it represents an alternative and rapid way for new blood vessel production, that permits rapid density increase of capillary vascular bed[56].

Next to vasculogenesis and angiogenesis, several other mechanisms of neo-vascularization have been recently identified in tumors, among these: vessel co-option and vasculogenic mimicry[56]. Vessel co-option is the mechanism by which tumors can grow in avascular stage, without inducing tumor vessel production, taking advantage to host vessels[56]. This may happen in tumors of well-vascularized tissues, like brain and lung, where cancer cells can grow along existing vessels without evoking an angiogenic response. Vessel co-option has been shown as a strategy employed by some glioblastoma (GBM) cells to invade further into the brain, leading to one of the greatest challenges in treating GBM[57]: the systemic anti-angiogenic treatment of a GBM with an anti-VEGFR2 antibody was able to reduce tumor angiogenesis but led to an increased co-option of host vessels in the brain[58], emphasizing the need for treatment able to prevent both angiogenesis and vessel co-option. Vasculogenic mimicry was introduced to describe the masquerade of tumor cells as ECs[45]. This process of cell plasticity occurs mainly in aggressive tumors in which cancer cells de-differentiate to an

endothelial phenotype and make tube-like structures. This mechanism provides tumor cells with a secondary circulation system of vasculogenic structures lined by tumor cells, independently of angiogenesis[44]. This phenomenon was described for the first time in melanomas[44] but recently has been associated with small cell lung cancer, breast cancer[59] and gastric carcinoma[60]. The recent finding elucidates the clinical implication of vasculogenic mimicry even in Pancreatic Ductal Adenocarcinoma (PDAC) progression[61], often associated with poor prognosis. Accordingly, the disappointing results of clinical trials focused on anti-angiogenesis therapy in PDAC, give us novel insights into other functional vessel-like forms that underlie the perfusion of tumors[45]. The idea that these structures could form a functional secondary vascular network independently from angiogenic growth factors, makes tumor growth inhibition even more complex.

Tumor vessels originate through all the biological processes described above, that may occur simultaneously or at different times. All these mechanisms vary between tumor types and the surrounding environment, but they are all orchestrated by a range of secreted factors and signaling pathways, activated following the decrease of local O_2 level.

1.2 The non-cellular components of TME

An important aspect of TME is the ECM surrounding tumors, an highly dynamic structure that comprises a meshwork of polymeric proteins and accessory molecules, and provides structural and biochemical support for tumor growth[15]. Reciprocal communication between cancer cells and ECM defines important aspects of cancer progression, even if there is still poor knowledge about the mechanisms involved. What is known is the plasticity of cancer cells, defined as their ability in modifying themselves in order to survive the hostile TME and resist cancer therapies[62]. ECM composition varies depending on the resident tissue but in general it includes macromolecules (glycoproteins, collagens, enzymes), ligands and signaling molecules (cytokines, secreted proteins, growth factors), adhesion proteins (such as integrins), small RNAs, DNA, metabolism products such as ATP and its catabolites, and the solid-state of ECM that renders TME very suitable for tumor progression[62]. All these elements compose an active tissue providing both bio-physical (e.g., increased extracellular stiffness, shear stress) and bio-chemical (e.g., hypoxia, acidosis and ATP accumulation) stimuli that directly act on cancer and stromal cells, thus affecting different

steps of tumor progression, including angiogenesis[22].

Tumor ECM undergoes continuous remodeling by cancer cells themselves or stromal cells, and this, together with the high interstitial pressure generated within tumors, acts as important mechanical stimulus on tumor vessels[22]. ECs take advantage of the interconnected mechanosensory networks, including cytoskeleton, membrane proteins (integrins, cell-cell adhesion receptors, ion channels, receptor tyrosine kinases, G-protein coupled receptors) and transcription factors[63], to convert mechanical forces and biophysical cues in signaling pathways responsible of specific cellular responses[22,63]. For example, increased ECM stiffness has been demonstrated to modulate VEGFR-2 expression, via a mechano-sensitive signaling transduction pathway that tunes the balance between TFII-I and GATA2 transcription factors[64], and to promote sprouting angiogenesis and vascular permeability[65] by altering the VE-cadherin localization[66] during capillary formation.

The reduction of physiological O_2 levels, known as hypoxia, characterizes the great majority of malignant tumors and has strong impact on angiogenesis[34]. The aberrant vascularization and poor blood supply previously described, lead to transient (acute) or permanent (chronic) hypoxic conditions[67,68] in TME, each responsible of specific

biological reactions inside cancer cells. Chronic hypoxia activates the metabolic switch that leads to the preference of anaerobic glycolysis, responsible for the genetic instability and the acquisition of the malignant phenotype (invasiveness and metastasis ability) of cancer cells. The increased O_2 demand for growing tumors, leads to the angiogenic process and formation of structurally and functionally abnormal blood vessels[69], responsible for the inefficient blood perfusion that results in acute hypoxia. Tumor-associated hypoxia stimulates a complex cell signaling network in cancer cells (activation of HIF, PI3K, MAPK, and NFκB pathways), causing both positive and negative feedback loops that consequently enhance or diminish the hypoxic effects[67,70–72]. One of the main outcomes of the HIF-dependent signaling is, in fact, the expression of growth factors and cytokines (VEGF, EGF, SDF-1α) implicated in delivering sustained pro-angiogenic signals to both ECs and EPCs, the former residing in close proximity to the primary tumor and the latter recruited to the sites of neo-vascularization[73], in order to stimulate the acquisition of abnormal proliferative and migratory capabilities[35,40,48].

In addition to hypoxia and the consequent metabolic switch in cancer cells, poor vascularized tumor regions lead to a buildup of toxic waste products, such as lactate, resulting in acidosis. In

this context the so-called "Warburg effect" plays a crucial role: it relies on mitochondrial dysfunction and is characterized by respiratory impairment and switch to glycolysis, providing glucose consumption and lactate secretion[74,75]. Interestingly, this metabolic way is preferentially chosen by cancer cells even in adequate O_2 conditions and it can be linked to a reduced expression of tumor suppressor gene p53 in cancer cells[75]. In order to maintain the intracellular pH, cancer cells regulate the expression of proteins which pump out hydrogen ions (H^+) such as the sodium/protons (Na^+/H^+) exchanger transporter–isoform 1 (NHE1), whose activation in tumor cells is mainly due to several soluble growth factor stimulation, low serum and hypoxia[76]. NHE1 is a reversible antiporter that uses energy provided by Na^+ gradient to expel H^+ with the final outcome of extracellular acidification (pH = 6.2 - 6.9), one of the main pathophysiological traits of solid tumors[74,77]. Interesting, has been shown that in breast cancer the higher invasiveness and metastasis activity of primary tumor is due in part to the interaction between CD44 (a cell-surface glycoprotein involved in cell adhesion and migration) and NHE1[76,78]. ECs was shown to activates in response to acidosis with the purpose to resolve tissue acidification by stimulate neo-angiogenesis. This may happens possibly by two

ways: (I) the lactate internalization, via lactate importer monocarboxylate transporter 1 (MCT1), and the activation of NFkB pathway[40], and (II) the proton-sensing GPR4 receptor-induced inflammatory response[79] that triggers pro-angiogenic factors release. However, the molecular mechanisms by which ECs sense and react to the acidic TME are not fully understood. In this context, the involvement of pH-sensitive ion channels, among which there are the most thoroughly studied TRP vanilloid-1 (TRPV1)[22], other TRP family members (TRPV4, TRPC4, TRPC5, TRPP2)[22], the store operated channels (SOCs)[80] and some members of ionotropic purinoceptors (e.g., P2X2, P2X4, P2X7)[6], may play an interesting role. Most of them are Ca^{2+}-permeable channels usually expressed in ECs but whether and how extracellular acidification affects the intracellular Ca^{2+} signaling and accordingly modify some functional ECs responses, is still an open question.

Plasma membrane ion channels represent very suitable and interesting target to study the interaction between ECs and TME since they convert extracellular biophysical (mechano-sensitive ion channels) and/or biochemical (pH or hypoxia modulated ion channels) cues in intracellular signaling pathways responsible of specific cellular response.

1.2.1 Extracellular ATP accumulation

TME is characterized by the accumulation of ATP and other nucleotides and nucleosides, that affect not only tumor growth but also immune cells functions and tumor-host interaction[3,81]. ATP that accumulates in TME acts as a signaling molecule through the binding with purinergic receptors (PRs) located on the surface of cancer and stromal cells[81], thus participating to the purinergic signaling pathway.

Nowadays, growing consensus regards ATP and adenosine (ADO) as TME hallmarks. Extracellular ATP (eATP), in fact, reaches concentrations much higher than those measured in healthy tissues[81–84] (tens of nanomolar vs. hundreds of micromolar) and its total amount strictly depends on the balance between its release by different cell types and its breakdown into ADP and ADO by ectonucleotidases[85–88]. CD39 and CD73 are the major ectoenzymes expressed by cancer cells, immune cells and ECs[89,90]. CD39/ecto-nucleoside triphosphate diphosphohydrolase-1 (ENTPDase1) drives the sequential hydrolysis of ATP and ADP to AMP while the formation of ADO from AMP is accomplished primarily through CD73 (ecto-5-nucleotidase), a glycosyl phosphatidylinositol-linked membrane protein[91].

Tumor-associated eATP accumulation mainly derives from stressed and dying cells that release ATP as pro-inflammatory danger signal and inflammatory cells, once reached the tumor site, further contribute to the release of ATP[92]. Besides these major source of ATP, other different mechanisms contribute to the high eATP accumulation in tumor tissues[2,81,84], e.g. hypoxia itself is a strong stimulus even in absence of cell injury[70,93]. The electrochemical gradient of ATP molecules actively contribute to the ATP extrusion from the cells: the concentration range of intracellular ATP is around 5–10 millimolar versus the low nanomolar levels typical in healthy tissues and the two negative charges carried by a single ATP molecule, considering the presence of extracellular physiological divalent cation concentrations (such as calcium – Ca^{2+}), create the outward-directed ATP gradient[94]. In addition to the passive efflux, cells actively release ATP through vesicle exocytosis[95] and non-selective pores, such as connexins, pannexin-1 (Panx-1)[96–98] and the purinergic ionotropic receptor P2X7[95]. Panx-1 represents a versatile and tunable partner in purinergic signaling because it feedbacks inhibition through the low affinity binding with ATP, in the extracellular domain. This mechanism is thought to be the major pathway for ATP efflux, not only in cancer cells[99], and represents optimal way to avoid

excessive and potentially dangerous ATP accumulation in the pericellular space[100].

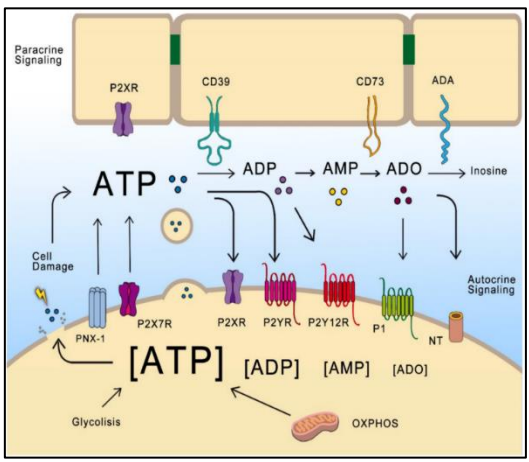

Figure 3. Schematic representation of purinergic nucleotides and nucleosides acting as autocrine and paracrine messengers. In cancer, ATP can be released to extracellular space by cellular lysis, exocytosis, transporters, hemichannels of pannexin-1 and P2X7R. Once located at the extracellular space, ATP activates P2XR and P2YR and can be hydrolyzed by ectonucleotidases (CD39 and CD73) to form ADP, AMP and ADO.
Campos-Contreras et al., Cells, 2020.

2. Purinergic Signaling

PRs are a super-family of membrane receptors of which ATP, its catabolites and other nucleotides, are the natural agonists. They are classified into two major families: P1 receptors (P1Rs), the metabotropic receptors endogenously activated only by adenosine (ADO), and P2 receptors (P2Rs), activated by a wide spectrum of nucleotides and nucleosides[4]. P2Rs are further divided into two sub-families: the ionotropic P2X receptors (from P2X1R to P2X7R) and the metabotropic P2Y receptors (P2Y1R, P2Y2R, P2Y4R, P2Y6R, P2Y11R, P2Y12R, P2Y13R and P2Y14R)[101,102]. Generally, the downstream functional effect following their activation depends on the subsets of PRs expressed by the cell[4].

Different cellular processes are regulated by extracellular nucleosides and nucleotides: they participate in stimulation (or inhibition) of cell proliferation, migration, differentiation, death and secretion of inflammatory mediator and growth factors[103]. PRs widespread tissue distribution causes their implication in a diverse range of physio-pathological processes[104] (like pain sensation[105,106], neurotransmission[107,108], inflammation[109]) including cancers[110] and growing interest has been focused on the therapeutic potential of purinergic signaling[11183].

Purinergic signaling in cancer mainly refers to adenine nucleosides (ADO) and nucleotides (ATP and ADP). This is probably due to the much wider activity spectrum of purine versus pyrimidine: ATP activates all P2Rs, while UTP, UDP and UDP-glucose can only bind and activate four out eight P2YRs subtypes and none P2XRs[3]. Many malignancies overexpress several P1Rs and/or P2Rs subtypes[3,83,112] and are not surprising the therapeutic approaches aim to block them in order to suppress tumor growth. Since P1Rs, P2Rs and ATP/adenosine-degrading enzymes are expressed by cancer cells as well as by the host immune and stromal cells, additional powerful novel anti-cancer combination therapies might come from targeting PRs in association with modulators of extracellular adenosinergic pathways[91,113]. In this context, targeting P2X7R obtained proved efficacy in several preclinical tumor models, as well as CD39 and CD73 enzymes that represent interesting targets in both tumor and immune cells, highlighting the therapeutic value of a combination therapy[91,113].

Purinergic signaling has been well studied in cardiovascular system, where it plays pivotal role in controlling vascular tone and remodeling[114]. In physiological conditions (intact endothelial monolayer), ATP released by shear stress acts on endothelial P2Rs to elicit vasodilatation, via the

release of NO[115,116]. On the contrary, in presence of endothelial damage, ATP may act as a vasoconstrictor via P2Rs on the vascular smooth muscle, which may lead to local vasospasm[87,101]. Different purinergic regulatory mechanisms involve different PRs subtypes in different blood vessels and in different species: P2XRs expression and function in endothelium is not fully elucidated, their role in the regulation of cardiovascular system mainly refers to their expression in smooth muscle cells. However, P2X2R, P2X3R, and P2X4R have been associated with endothelium, appearing to be involved in cell adhesion and gap junction formation[117–120]. ATP and its catabolites control also several acute vascular functions involved in the angiogenic process[86–88,121–123], such as cellular proliferation and migration, through the activation of intracellular protein kinases, including the p42/44 MAPK, c-Jun N-terminal kinase (JNK), PI3K/Akt, ERK 1/2, that may underlie the sustained effects of ATP in ECs and smooth muscle.

As aforementioned before, the potential efficacy of purinergic signaling in the treatment of cancer has recently been evaluated[115] but remains still debated its role in tumor vasculature[3,81,83]: very few studies are currently available about the effects of purinergic stimulation in tumor endothelium.

2.1 The Metabotropic P1 and P2 Receptors

The metabotropic P1Rs are also named Adenosine Receptor (ARs) and comprise a group of G protein-coupled receptors (GPCRs). To date, four subtypes of ARs (A1, A2A, A2B and A3) have been identified, each with different localization, signal transduction pathways and functional significance upon exposure to the agonist[4]. The role of ADO in cancer is controversial: depending on the cancer type and the P1R involved, it may play pro- or anti- tumor activity[124]. P1Rs molecular structure includes seven α-helical structure transmembrane (TM) domains with an extracellular amino-terminus (N-term) and an intracellular carboxy-terminus (C-term)[125,126]. The *N*-term domain has *N*-glycosylation sites which influence the trafficking of the receptor to the plasma membrane, while the C-term contains serine and threonine residues that serve as phosphorylation sites for protein kinases and enable receptor desensitization[125,126]. Furthermore, the C-term and the third intracellular loop, enable coupling to G proteins[125,126]. The A1 and A2A receptors possess a high affinity for ADO while A2B and A3A receptors show relatively lower affinity. P1Rs have traditionally been classified based on their differential coupling to Adenylyl Cyclase (AC): A2A and A2B are coupled to G protein with alpha

subunits stimulating AC (Gαs), therefore activating protein kinase A (PKA) to phosphorylate the Cyclic AMP (cAMP) Response Element Binding protein (CREB); on the contrary, A1 and A3 receptors are coupled to G protein with alpha subunits inhibiting AC (Gαi) and their activation inhibits cAMP production and decreases PKA activity and CREB phosphorylation[127,128]. P1Rs show also different desensitization mechanisms: A1R is phosphorylated and internalized slowly (several hours), A2AR and A2BR demonstrate a more rapid down-regulation (an hour), and A3 down-regulation and desensitization occurs within minutes[129].

Human P2YRs are GPCRs with a molecular structure that resemble those of P1Rs: seven α-helical TM domains, an extracellular N-term (containing potential glycosylation sites) and an intracellular C- term (containing possible binding/phosphorylation sites for protein kinases)[130]. One possible classification of P2YRs subtypes is based on their pharmacological profile: P2Y1, P2Y11, P2Y12 and P2Y13 are purine-selective receptors; P2Y4, P2Y6 and P2Y14 are pyrimidine-selective receptors[130]. More in detail, ATP preferentially activates P2Y11 while ADP and its analogues mainly act on P2Y1, P2Y12 and P2Y13. UTP and UDP mainly bind with P2Y4 and P2Y6 respectively, while UDP-glucose is the preferential agonist of P2Y14[130]. The exception to

this classification is represented by P2Y2, which is activated by both ATP and UTP with approximately equal potency[131]. The classical P2YRs antagonists are suramin, that antagonizes most P2YRs receptors but not P2Y4, pyridoxal-phosphate-6-azophenyl-2",4"-disulphonic acid (PPADS), that strongly antagonizes P2Y1 and weakly blocks other P2YRs, and reactive blue 2 (RB-2)[132]. The second possible classification of the P2YRs family is based on their coupling with G protein. According to this, P2Y1, P2Y2, P2Y4, P2Y6 and P2Y11 couple to the (pertussis-toxin-resistant) G q (Gαq) protein with alpha subunit directly activating phospholipase C–β (PLC-β), while P2Y12, P2Y13 and P2Y14 belong to the (pertussis-toxin-sensitive) Gαi protein-coupled subfamily[133,134]. However, the real situation is even more complex: individual P2YRs may couple to functionally distinct heterotrimeric G proteins, as well as to monomeric small GTPases[134].

2.2 The Ionotropic P2X Receptors

Human P2XRs sub-family consists of seven (from P2X1 to P2X7) membrane cation-permeable and ligand-gated channels that open in response to the binding of ATP[135]. Three P2X subunits assemble by forming the central pore, giving rise to a homo- or hetero-trimeric ionotropic

receptor[136,137]. There are three ATP binding sites, located at the interface between subunits, meaning that three agonist molecules are needed to activate the receptor[138]. All P2XRs are selectively activated by ATP, much less activated by ADP, and not activated at all by AMP, ADO or other purines (e.g., GTP) or pyrimidines (e.g., UTP and CTP)[135]. However, each P2XR family subtype shows subtle biophysical and/or pharmacological differences. In general, upon the binding with their ligand molecules, they open within few milliseconds, lead the passage of cation (preferably Na^+, K^+ and Ca^{2+}) through the membrane, and close within tens of milliseconds, when the application is discontinued (deactivation)[139]. Ionic currents through P2X1 and P2X3 receptors decline during the application of ATP (desensitization) within tens or hundreds of milliseconds, for P2X2, P2X4 and P2X5 receptors, ionic current decline occurs slowly, in seconds or tens of seconds, and for P2X7, there is little decrease in the current even over several minutes (slowly or non-desensitizing receptor)[139]. Actually, P2X7 shows further peculiarity that will be discussed in the following paragraphs.

P2X subunits are proteins ranging from 379 (P2X6) to 595 (P2X7) amino acids with cytoplasmic N- and C-term, possessing consensus binding motifs for protein kinases and two TM-spanning regions (TM1 and TM2)[140]. TM domains are

involved in receptor heteromerization and connected by a large extracellular loop, with ten conserved cysteine residues forming a series of disulfide bridges[138]. Binding with ATP causes subunits to flex together within the ectodomain and separate in the membrane-spanning region and open a central pore for ion flow[140]. TM1 is involved with channel gating and TM2 lining the pore[140]. Of the subunits, the C-term domain is the least-conserved part in the amino acid composition, ranging in length between 27 (P2X6) and 239 (P2X7) amino acids, indicating that it might confer subunit-specific properties; it contains several residues playing important roles including receptor trafficking[141], determine the desensitization rate and direct physical interactions with cysteine-loop receptors. Both N- and C-term are targets for post-transcriptional modifications, RNA splicing, phosphorylation, and protein–protein interactions with other receptors or regulatory molecules[132]. These modifications and interactions, together with hetero-trimerization or multimerization of P2X subtypes, may critically influence channel functions and certainly confer great variability to the P2X-mediated cell responses. The heteromerization of different P2Xs subunits may create ion channels with different biophysical and/or pharmacological characteristics from the homomeric form,

challenging the PRs profile characterization in cellular models.

P2XRs emerged as central players in different steps of tumorigenesis. They were found expressed and functional in both tumor and stromal cells, but further elucidation about their involvement in angiogenesis is still required. In this light, next paragraphs aim to clarify which P2Xs agonists or antagonists should be used to target and distinguish P2Xs members from each other.

2.2.1 Pharmacology of P2X Receptors

As mentioned earlier, ATP is the general and natural agonist of each P2XR, although it shows different potency profile. The EC_{50} values for ATP range from sub-micromolar concentrations for P2X1, P2X3, and P2X5 to low micromolar concentrations for P2X2 and P2X4. At P2X7, EC_{50} values for ATP range from about 0.1 to 1 millimolar while Benzoylbenzoyl-ATP (BzATP) is at least one order of magnitude more potent than ATP, even if it has also considerable activity at other P2X isoforms[142]. All P2Xs agonists known so far are nucleotide analogs and among these ATP-γ-S and α,β-MethyleneATP (αβ-meATP) are the most metabolically stable (i.e., do not undergo degradation by surface-located ectonucleotidases) and widely used to investigate ATP-gated channels

in native tissues[143]. P2X7 represents an exception resulting not readily activated by αβ-meATP (EC_{50} >> 100 μM). Other P2Xs agonists are 2-Methylthio-ATP (2-meSATP) and diadenosine polyphosphates (Ap3A and Ap4A)[140]. All these P2X agonists may activate also some P2Y family members, but with different potency profiles, as well as conventional antagonists like suramin, PPADS and RB-2, that are not subtype-specific and block several P2X and P2Y subtypes[140]. Brilliant Blue G (BBG) and Oxidized ATP (oATP) are usually used as P2X7 antagonist (the latter requires extensive pre-incubation)[140]. In this light, more specific (NF compounds) and potent (MRS compounds) antagonists have been developed and during the last two decades, also new types of mostly non-nucleotidic and subtype-specific antagonists (such as the P2X7-selective A-438079, A-740003, AZ 11645373, etc.) have been developed[140]. These efforts mainly focused on P2X3 and P2X7 subtypes that appeared to be the most relevant drug targets.

To date, eight functional heteromeric P2XRs with pharmacological and/or biophysical properties that differ from the individual subunits have been identified: P2X1/2, P2X2/3, P2X1/4, P2X1/5, P2X2/5, P2X2/6, P2X4/6 and possibly P2X4/7[144]. In these heteromers, the kinetic and ligand-binding properties of the constituting

subunits are combined. Generally, slowly desensitizing subunits dominate the kinetic, while subunits with higher affinity for agonist and/or antagonist appears to increase the sensitivity of the heteromer for the respective ligand. For example, in heteromeric assemblies, P2X1, P2X3, P2X5, or P2X6 subunits appear to confer αβ-meATP sensitivity to the receptor[144–146]. The often slightly lower potency of agonists at the heteromers is too subtle for true discrimination: e.g., is difficult to discriminate heteromeric P2X1/P2X3R from the P2X1R or P2X3R, even if they most likely reflect a lower affinity for ATP at the heteromeric ATP-binding sites. For this reason, no selective compounds for any of the heteromeric receptors has been identified[147,148]. Despite this, using some compounds is still possible to discriminate between homomeric and heteromeric P2XRs[149–151]: e.g., P2X2/P2X5 heteromers have slightly reduced sensitivity to ATP, ATP-γ-S and BzATP, a strongly reduced efficacy of BzATP is observed and αβ-meATP is ineffective at concentrations of 300 μM[143]. Interestingly, different molecules acting on homomeric receptors lose their affinity at the heteromeric form, despite at least one P2X-P2X interface of the same P2X subtype is maintained. Possible explanations for this discrepancy would be that the P2X-P2X interface is markedly altered by the inclusion of a single different P2X subunit in

the complex and/or that occupation of one interface is insufficient and more than one ligand has to bind to produce an efficient channel block[143].

2.2.2 The Allosteric Modulators of P2Xs

P2XRs differ from other ligand-gated ion channels in having three inter-subunit ion access pathways that widen during channel opening[152]. This, in combination with the high flexibility of the ectodomains and their linkers to the TM domains, might enable P2XRs to tolerate or compensate more or less pronounced antagonist or channel allosteric modulators that induce conformational changes before a complete channel block[6]. The ATP binding pocket at the ectodomain appears also to form sites for antagonists and modulators[153] including cations such as Ca^{2+} and H^{+} but also magnesium (Mg^{2+}), zinc (Zn^{2+}) and copper (Cu^{2+})[154].

Modulation by proton (H^{+}) has been well studied in P2Xs since their well knows acid-sensitivity. All the homomeric P2Xs are inhibited by acidic pH, except for P2X2, where acidification enhances response of agonists and the antagonist suramin[6]. The recurrent target for H^{+} binding are non-protonated carboxylic acid residues or extracellular histidines (His), in particular, the putative extracellular pH sensors are His319 for

P2X2, His206 for P2X3 and His286 for P2X4. Proton-modulation of P2X7 has been shown to involve both His130 and Asp197[7]. In the heteromeric forms of P2Xs, modulation by H^+ seems to be more complex[155,156]: for example, P2X1/2R shows novel pH sensitivity, resulting in increased agonist potency at both acidic and alkaline pH[155], that differs from homomeric P2X1 and P2X2.

One of the most remarkable characteristics of P2Xs is their differential allosteric modulation by metals. Several amino acid residues, probably part of specific metal allosteric sites, have been identified as crucial for metal effects, that vary among different metals and different P2Xs. The first allosteric modulators described for P2XR family were the trace metals Zn^{2+} and Cu^{2+}, both of them used also as additional criteria to characterize P2XRs. Zn^{2+} and Cu^{2+} allosterically modulate P2Xs in complex subtype- and species-specific ways and via non-conserved binding sites[6]. Briefly, Zn^{2+} inhibits P2X1 and P2X7 while modulates P2X2, P2X3, P2X4, and P2X5 currents in a biphasic way (i.e., it potentiates at low concentrations and inhibits at high concentrations). Biphasic modulation of these receptors suggested the possible existence of two allosteric sites: high-affinity with positive modulator effect and low-affinity site with negative modulator role[150]. P2X2

and P2X7 reveal a species-specific modes of metal modulation[157]: opposite role for Zn^{2+} modulation was observed in rat and mouse compared to human P2X2 (the latter is inhibited by Zn^{2+} and Cu^{2+} [157–159]); both Cu^{2+} and Zn^{2+} attenuated ATP-gated current in rat P2X7 but only Cu^{2+}, and not Zn^{2+}, inhibits the mouse receptor[160]. Interestingly, the Ca^{2+} influx through recombinant mouse P2X7, is potentiated by Zn^{2+} when activated by ATP but inhibited when stimulated with BzATP[160].

As well as Cu^{2+} and Zn^{2+}, divalent cations like Ca^{2+} and Mg^{2+} exert a modulator role on P2XRs. Both of them, inhibit P2X7 activity[8] while Mg^{2+} was shown to directly inhibit also P2X1 and P2X3. Orthosteric agonist potency at P2X7 decreases if Ca^{2+} or Mg^{2+} are present in the recording solution: Ca^{2+} acts as an allosteric inhibitor[161], independently of the free agonist concentration, while Mg^{2+} inhibition seems to be due to both an inhibitory Mg^{2+} binding site and a lower or absent agonist activity of Mg^{2+}-bound ATP at the P2X7[5,8,162]. Differences in the sensitivity to free ATP and Mg^{2+}-bound ATP were also reported for P2X2 and P2X4[163].

Interestingly, the widely used antiparasitic agent in human and veterinary medicine Ivermectin (IVM)[164], extends the growing list of species-specific P2X7 modulators. It gains interest as P2X4 modulator[165–172] but it has been also shown to

potentiate human P2X7-mediated Ca^{2+} influx, probably hindering the closure of channel pore[173].

Further elucidation about the mechanisms of modulation of P2Xs and the possible consequences in their functionality, including the activation of specific intracellular pathways, will certainly open promising opportunities in studying how cells interact with environmental cues by modify certain functions.

2.2.3 The Peculiar P2X7R

Among P2XRs, P2X7 shows unique features that make it the most intriguing member of the whole P2Xs family. First of all, is well known its complex gating behavior in which the permeation pathway, during several seconds of ATP application, dilates from a pore that only allows the passage of small cations to one that allows permeation of larger cations (such as *N*-methyl-D-glucamine) and dyes (such as ethidium and YO-PRO-1)[174]. Then, it differs structurally in the long intracellular C-terminal tail[96] and pharmacologically in its low affinity towards ATP (EC_{50} > 100 μM)[175]. The availability of chicken and mammalian P2X7 crystal structures shows that functional P2X7 three-dimensional monomer could be compared to the shape of a dolphin[152] and provide information about the most largely used agonist and antagonists

binding sites[176]: ATP binding to the receptor in the range of milliseconds triggers the small cation-selective pore opening; prolonged ATP exposure (range of seconds) results in the larger pore (macropore) formation, allowing molecules up to 900 Da to flow and eventually leading to cell death by apoptosis or autophagy[177,178]. Nowadays, the molecular mechanisms responsible for the large molecules efflux through P2X7 is still a controversial argument[176,179].

Although previously P2X7 was thought to be unique in not forming functional heteromers, nowadays we known that P2X4/7R is expressed by immune cells[180] and interesting studies on P2X2/5R revealed that it may resemble the biophysical profile of P2X7R and activates similar cellular responses[181]. In fact, P2X2/5R permeability changes in ATP-activated and time-dependent manner, showing the large conductance channel conformation, previously associated only with P2X7R. Remarkably, HEK cells co-expressing P2X2 and P2X5 subunits displayed plasma membrane blebbing and flipping of phosphatidylserine (PS) from the inside to outside surface, two hallmarks of P2X7R[181].

Moreover, P2X7 significantly contributes to increase the great variability within P2Xs: it is highly polymorphic, with more than 150 non-synonymous Single Nucleotide Polymorphisms (SNPs), of

which at least eight are loss-of-function[96], and it has been associated with ten splicing variants (P2X7A-J). Some splicing isoforms give rise to receptors with altered channel functionality, for example P2X7B isoform, which shares the similar predominant tissue distribution of the canonical full-length P2X7A but lacks the macropore function while maintaining channel activity[96]. Noteworthy, some non-functional P2X7Rs (nfP2X7Rs) are described in the literature as preferential cancer-related isoforms[182,183], probably due to their inability to form the macropore thus conferring more resistance to apoptosis. P2X7R SNPs and alternative splicing isoforms are gaining huge interest in relation to human health and disease[184,185].

Many studies point to a critical role of P2X7R-dependent signaling in different physiological and pathological processes, including cancer[111]. P2X7R is considered as a key mediator of anti-tumoral immune response[186] and it is present at the surface of most tumor types[187], thus establishing a powerful links with different stages of tumor progression, including angiogenesis. Moreover, P2X7R stands out among P2Xs because of its validated pro-angiogenic role in tumors: its over-expression in cancer cells promote the release of VEGF and proteases (by cancer and stromal cells) promoting both angiogenesis and metastasis spreading[188,189].

ATP accumulated in TME activates P2X7R in a specific manner (considering its low sensitivity towards ATP) and was shown to increase cancer cells proliferation and migration in glioma[190], breast cancer[191] and PDAC[192]. This downstream functional effect of P2X7R has been shown to be mediated by the activation of different intracellular pathways, e.g., the activation of PI3K/AKT and ERK1/2 in breast and prostate cancer[193,194] or the activation of ERK 1/2 and c-Jun N-terminal kinase (JNK) in pancreatic cancer[195]. In this light, not surprising are the large number of studies showing the possibility to use P2X7R antagonists and inhibitors to reduce tumor growth and cancer cells migration, proliferation and invasion[176] but, in order to improve the chances in render P2X7R a feasible drug target for the treatment of cancer, is necessary to consider the context in which it works, that is the potential effects of TME on its functionality.

As aforementioned, noteworthy studies report the modulation of P2X7R activity by different factors typically considered TME cues: low pH (widely described in previous paragraph), hypoxia and increased ECM stiffness[196]. Conflicting data regard hypoxia effect on P2X7R expression: in cancer cells from GBM hypoxia has been showed to promote up-regulation of P2X7 with following nuclear translocation of NF-$\varkappa$B, promoting tumor cell invasion[10]; on the contrary, P2X7 down-

regulation was observed in breast cancer cells exposed to hypoxia[9]. Interesting, has been also shown that P2X7 mediates upregulation of HIF-1α in astrocytes (conferring increased ischemic tolerance to the cells)[197,198] while in GBM, P2X7 down-modulation correlated with reduced HIF-1α levels[199]. Recently, P2X7R has been also recognized as mechano-gated ion channel, although indirect, i.e., through the involvement of Panx-[12]. Panx-1 is the mechanosensitive channel releasing ATP into the extracellular space (in response to shear stress or increased osmotic pressure) which then binds and activates P2X7R[11]. Panx-1 is often associated with P2X7R expression and appears as key elements in macropore formation upon prolonged ATP application on P2X7R[200].

As previously described, P2X7R over-expression in cancer cells promotes cells proliferation and migration but actually, this pro-tumoral activity may be counteract by the ability to trigger apoptosis through the macropore formation. Indeed, the preferential expression of a nfP2X7R give rise to cancer cells often over-expressing P2X7R[183,201]. Another feedback inhibition mechanism to hamper the macropore formation is mediated by MMP-2[202]. These elements render P2X7 a versatile ion channel, which modifies its functional characteristics according to the survival needs of the cell.

3. Ca^{2+} Signaling

Ca^{2+} is a versatile intracellular messenger. This versatility is exploited to control different processes from cell proliferation to cell apoptosis and is provided by many components, being part of the "Ca^{2+} signaling toolkit", that can be mixed and matched to create a wide range of spatial and temporal intracellular Ca^{2+} signals[203]. The finely tuned intracellular Ca^{2+} mobilization is due to the very low (nanomolar range) resting cytosolic free Ca^{2+} concentration ($[Ca^{2+}]_c$), compared with the extracellular free Ca^{2+} (millimolar range) and intracellular Ca^{2+} stores (micromolar range)[203].

Once Ca^{2+} carried out its signaling functions, it is rapidly removed from the cytoplasm by various pumps and exchangers: the plasma membrane Ca^{2+}-ATPase (PMCA) pumps and Na^+/Ca^{2+} exchangers extrude Ca^{2+} to the outside whereas the sarco-endoplasmic reticulum ATPase (SERCA) pump returns Ca^{2+} to the Endoplasmic Reticulum (ER), the main intracellular Ca^{2+} reservoir[203]. Besides ER, other organelles act as Ca^{2+} reservoirs, also in ECs: lysosomes, the Golgi apparatus and mitochondria. Active transport of Ca^{2+} inside organelles and outside the cell is part of the "off mechanisms" of the Ca^{2+} signaling toolkit that reduces the $[Ca^{2+}]_c$ by either sequestering

(Ca^{2+} buffers) or pumping it out of the cytoplasm, shutting down the Ca^{2+} response[203].

Intracellular Ca^{2+} mobilization is always triggered by stimuli of different nature. These stimuli largely depend on the activation of ion channels Ca^{2+} permeable in the plasma membrane or in ER, in both cases the result is an increase in the $[Ca^{2+}]_c$. Ca^{2+}-mobilizing signals include the four intracellular messengers inositol-1,4,5-trisphosphate ($InsP_3$), cyclic ADP ribose (cADP-r), nicotinic acid dinucleotide phosphate (NAADP) and sphingosine-1-phosphate (S1P)[203]. Among these, $InsP_3$ is an important intracellular second messenger: upon binding with $InsP_3$ receptors ($InsP_3R$) on ER, it elicits an increase in $[Ca^{2+}]_c$ due to the rapid passage of Ca^{2+} content from the ER lumen to the cytosol[204]. The resulting Ca^{2+} release and the subsequent decrease in ER luminal $[Ca^{2+}]$[205,206] trigger SOCE mechanism[204]. SOCE activates as a result of large fall in ER Ca^{2+} levels, when STIM proteins, the ER Ca^{2+} sensors, undergo a complex molecular rearrangement culminating in their oligomerization and translocation to ER-plasma membrane junctions, known as *puncta*[203]. Here, STIM binds to and gates SOCs, such as Orai1-3 channels and TRPC1-7, thereby trigging SOCE[207] that is the principal Ca^{2+} signaling pathway responsible for the Ca^{2+} entry in both excitable and non-excitable cells[208]. SOCE may be triggered by a

set of different membrane receptors[208], including P2YRs and has been shown to regulate tumor growth and metastasis in different cancer cell lines[207,209–212].

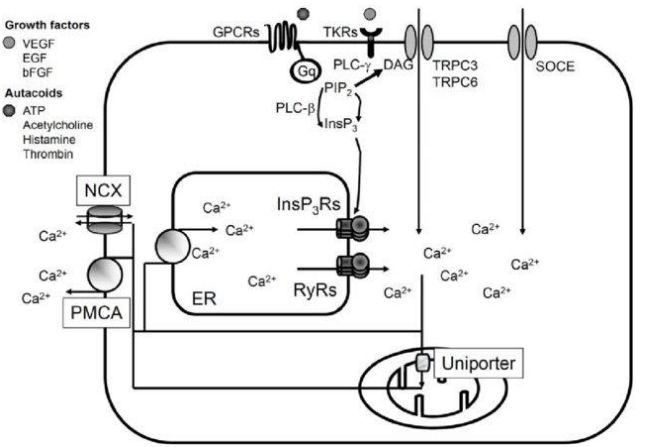

Figure 4. The Calcium Signaling toolkit in endothelial cells. Extracellular stimuli cause an elevation in intracellular calcium concentration through the activation of different membrane receptors: G-Protein Coupled Receptors (GPCRs), Tyrosine-Kinase Receptors (TKRs), ionotropic receptor. The following engagement of PLC-by GPCRs and PLC-by TKRs leads to PIP2 hydrolysis in InsP3 and DAG. InsP3 activates InsP3Rs to mobilize calcium stored within

the ER, while DAG stimulates calcium entry through the TRPC3 and TRPC6 non-selective cation channels. The InsP3-dependent fall in ER calcium levels results in the activation SOCE. Calcium levels return to pre-*stimulated* levels through the concerted action of the mitochondrial uniporter, SERCA and PMCA pumps, as well as through NCX.
Moccia et al., Anti-Cancer Agents in Medicinal Chemistry, 2014.

3.1 Purinergic Calcium Signals

As previously described, P2Xs are ion channel Ca^{2+} permeable located in plasma cells membrane and therefore, their activation lead pore channel opening and the subsequent direct influx of cations, among which Ca^{2+}, inside the cells. On the contrary, also P2Ys mediates the increase in $[Ca^{2+}]_c$ but they do in a different way, that is indirect.

Being GPCRs, P2Ys participate in regulate $[Ca^{2+}]_c$ basing on their coupling to G-protein. P2Y1, P2Y2, P2Y4, P2Y6 and P2Y11 couple to Gαq-protein and directly activates PLC-β family enzymes that lead the hydrolysis of phosphatidylinositol-4,5-bisphosphate (PIP_2) on the cell membrane with the production of $InsP_3$ and diacylglycerol (DAG)[130,203]. Either $InsP_3$ and DAG are important intracellular second messengers and essential regulators of $[Ca^{2+}]_c$[213], the former because it activates $InsP_3R$ on ER membrane and the latter because it is involved in the intracellular amplification cascade of Ca^{2+} signals[214]. P2Y12,

P2Y13 and P2Y14 couple to Gi-protein and also participate in regulating intracellular Ca^{2+} dynamics through the regulation of N-type Ca^{2+} channel activity[101,215].

Therefore, the activation of PRs triggers intracellular Ca^{2+} mobilization shaped by the direct Ca^{2+} influx through the membrane (P2Xs activation) and the $InsP_3$-dependent Ca^{2+} release from ER (P2Ys activation)[216].

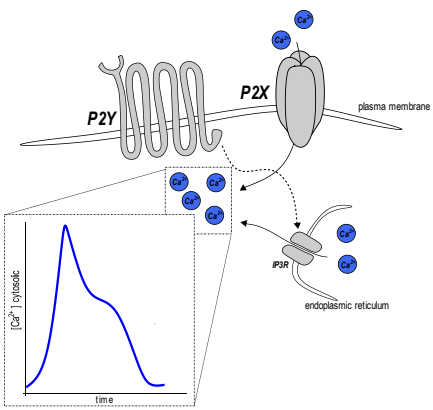

Figure 5. Schematic representation of purinergic-evoked intracellular calcium signals.
Activation of P2X receptors lead to a direct increase in the intracellular calcium concentration through the influx of calcium from the extracellular space to the cytosol. Activation of metabotropic P2Y receptors triggers intracellular calcium release through the activation of IP_3 receptors on the endoplasmic reticulum membrane.

3.2 Calcium Signaling in Cancer and Angiogenesis

Given the versatility of Ca^{2+} as intracellular messenger, not surprisingly abnormal regulations of Ca^{2+} homeostasis have been linked with different diseases including developmental disorders, hypertension, cardiovascular disease, diabetes, Alzheimer's disease and, of course, cancer[207,217].

The dysregulation of Ca^{2+} homeostasis has been suggested as an important event in driving the expression of the malignant phenotypes, e.g., the strict connection between enhanced cell migration (early prerequisite for tumor metastasis)[218–220] and the spatial and temporal organization of intracellular Ca^{2+} signals[221]. In this context, Ca^{2+} signals provide a rapid and robust way for the selective activation of signaling components that play a central role in cytoskeletal reorganization, traction force generation and focal adhesion dynamics[217]. Polarized and migrating cells exhibit a rear-to-front gradient of $[Ca^{2+}]_c$, with a higher concentration at the rear end of a migrating cell, which is thought to be responsible for rear-end retraction[222]. On the other hand, spatially and temporally confined repetitive changes in $[Ca^{2+}]_c$ (Ca^{2+} microdomains) are enriched near the leading edge of migrating cells and implicated in controlling cycles of lamellipodia retraction and strengthening

local adhesion to ECM[218–220]. The disassembly of cell adhesions is due to the cleavage of focal adhesion proteins, such as integrins, talin, vinculin and focal adhesion kinase (FAK), by the Ca^{2+}-dependent protease, calpain[223,224].

Several components involved in the extracellular Ca^{2+} influx pathway, including STIM/Orai-mediated SOCE, the Ca^{2+}-permeable TRPs and PRs family, have been implicated in cancer cell migration and tumor metastasis[51,207,210,217]. The overexpression of Ca^{2+} channels on plasma membrane increases Ca^{2+} influx and promotes pro-tumoral Ca^{2+}-dependent pathways (such as cell migration and invasion) or may represent an adaptive response that might offer a survival advantage to the tumor, such as resistance to apoptosis. In this light, not surprising are proteins part of the Ca^{2+} signaling toolkit, like Ca^{2+} channels and pumps, proposed as drug targets for cancer therapies. As mentioned in previous paragraphs, P2X7R may be a good candidate for cancer therapies given its often cancer cell-related over-expression and activation of Ca^{2+}-dependent pro-tumoral responses (enhanced cell migration and proliferation).

Ca^{2+} machinery is a potential molecular target for strategies against tumor neovascularization due to its multifaceted role in the control of endothelium homeostasis. Several studies

highlighted the importance of agonist-stimulated Ca^{2+} signals in angiogenesis and both pro- and anti-angiogenic molecules can induce a $[Ca^{2+}]_c$ increase often leading to different biological effects. Indeed, the role of $[Ca^{2+}]_c$ increase triggered by growth factors such as VEGF or basic fibroblast growth factor (FGFR) has been deeply investigated in ECs. Ca^{2+} entry triggered by VEGF, as well as by other pro-angiogenic factors, is often associated with an increase of vessel permeability, ECs survival/proliferation, migration and *in vitro* tubulogenesis[225]. As in activate mature ECs[226,227], recent studies show VEGF to stimulate EPCs through an oscillatory increase in $[Ca^{2+}]_c$[228–230]. Interesting, Ca^{2+} toolkit in EPCs derived from cancer patients is remodeled[231], thereby leading to the suppression of the pro-angiogenic Ca^{2+} response to VEGF.

Considering differences between normal and tumor vasculature, nowadays several patent applications aim to detect or interfere with $[Ca^{2+}]_c$ signals and their early downstream effects, especially in TECs without affecting normal endothelium[51]. In this light, Ca^{2+}-permeable channels often linked to tumor vasculature are the voltage-gated Ca^{2+}-channels (although ECs are generally described as non-excitable cells), the volume-regulated anion channels, nicotinic receptors and aquaporins[232]. Moreover, TRPV4

involvement in tumor angiogenesis is well established, although it is matter of debate whether its inhibition or activation is the best strategy for reducing angiogenesis[233,234]. However, arachidonic acid and its metabolites have been shown to enhance migration of TECs from breast cancer, through the activation of TRPV4 both directly and indirectly through the receptor trafficking to the membrane[234–236]. In the same model, nitric oxide and hydrogen sulfide have been demonstrated to trigger Ca^{2+} influx inducing cell migration[236].

The role of Ora1/STIM1 complex has been studied also in tumor vascularization, concurring to the VEGF-mediated SOCE in HUVEC[237]. ORAI1-mediated SOCE has been shown to drive colon cancer cell promotion of angiogenesis by hypoxia via a NOTCH1-dependent mechanism that involves the Ca^{2+}-dependent transcription factor NFATc3[238]. Besides hypoxia, another TME cue, the mechanical stretch, has been demonstrated to stimulate angiogenesis through the activation of Ca^{2+}-permeable channel Piezo2, in glioma[239].

Aim of the project

Previous work showed that high non-physiological eATP doses (> 20 μM) strongly inhibit the migration of ECs isolated from human breast carcinoma (BTECs) while no effect on NECs (HMECs) migration. Treatment with 100 μM ATP enhanced the attraction of human pericytes by BTECs, unveiling a potential pro-normalizing effect of purinergic stimulation[14]. Considering that eATP accumulation is one the hallmarks of TME and that purinergic signaling have been deeply investigated in cancer cells, further investigations about its role in tumor endothelium could be useful to enhance the comprehension of the mechanisms regulating one important step of tumor progression, i.e., tumor vascularization.

Since little is known about the purinergic Ca^{2+} signals in TECs, in this thesis project we first studied the Ca^{2+} signaling toolkit activated by high ATP stimulation (100 μM) and then its possible correlation with the functional effect on BTECs migration. In the second part of the work, we mainly focused on the role of P2X7-ionotropic receptor, typically overexpressed and widely studied in cancer cells, in the purinergic-induced functional response in BTECs. P2X7R, in fact, was previously shown to be expressed in BTECs and among P2Xs

it is selectively activated by high ATP doses. Finally, we analyzed the correlation between P2X7R-mediated Ca^{2+} signals and the anti-migratory activity of purinergic stimulation in different models of TECs with particular focus on its potential modulation by the environmental conditions.

Results

1. ATP Triggers Calcium Signals in human Cancer-derived ECs

In order analyze the intracellular Ca^{2+} dynamics following purinergic stimulation in Breast Tumor-Derived ECs (BTECs) we treated cells with different ATP concentrations (1, 10, 100 μM) both in presence and absence of extracellular Ca^{2+}.

In presence of 2 mM Ca^{2+} in the extracellular recording solution, ATP stimulations evoked an increase in the $[Ca^{2+}]_c$ in the great majority of cells examined, shaped by an initial Ca^{2+} transient (peak) usually followed by a sustained long-lasting phase (plateau) (**Figure 6 A**). A quantitative analysis of Ca^{2+} signals was then performed, taking into account both the peak and plateau phases (see Materials and Methods for data analysis details), showing a dose-dependent amplitude of the ATP-evoked Ca^{2+} signals (**Figure 6 B**).

When 1, 10 or 100 μM ATP was applied in a Ca^{2+}-free extracellular recording solution (0 Ca^{2+}_{out}), only a dose-dependent transient spike was detectable (**Figure 6 C**). This allowed to hypothesize that, in accordance with the literature, ATP-evoked Ca^{2+} signals in BTECs, both at high and low concentrations, are due to the intracellular

Ca^{2+} release (probably the main actor in the peak phase of the signal) and the extracellular Ca^{2+} influx, the latter mainly related to the long-sustained phase of the signals that was completely abolished after the removal of extracellular Ca^{2+} (**Figure 6 C**). Quantification the 1, 10, 100 μM ATP-evoked Ca^{2+} response in 0 Ca^{2+}_{out} showed again a dose-dependent amplitude of the signals (**Figure 6 D**).

Therefore, we decided to carry out the subsequent experiments, aimed to better clarify the purinergic-induced Ca^{2+} signaling profile in BTECs, with the highest tested ATP concentration (100 μM) that is associated with quantitatively larger Ca^{2+} signals and, to a greater extent, with the previously reported functional effects on BTECs migration[14].

Interestingly, Renal Tumor-derived ECs (RTEC) (characterized in[240]), displayed a similar biphasic response to 100 μM ATP (**Figure 7 A**) and moreover, we observed that their migration, similarly to BTECs, was affected by 100 μM ATP treatment (**Figure 7 E**).

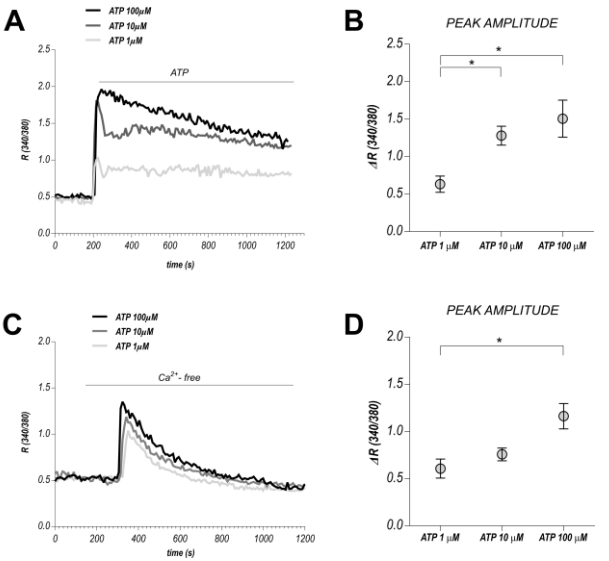

Figure 6. High eATP stimulation triggers biphasic Ca^{2+} signals in BTEC. (**A**) Representative traces of different Ca^{2+} signals evoked by three different eATP concentrations (1, 10, 100 μM) and (**B**) the relative quantification of the peak amplitude. Data are expressed as mean ± SEM. (**C**) Representative traces obtained upon 1, 10, 100 μM ATP stimulation in Ca^{2+} free extracellular medium and (**D**) the relative quantification of peak amplitude. Data are expressed as mean ± SEM. * p-value < 0.05; ** p-value < 0.005. Traces in A and C represent the average of all the cells in one representative experiment.

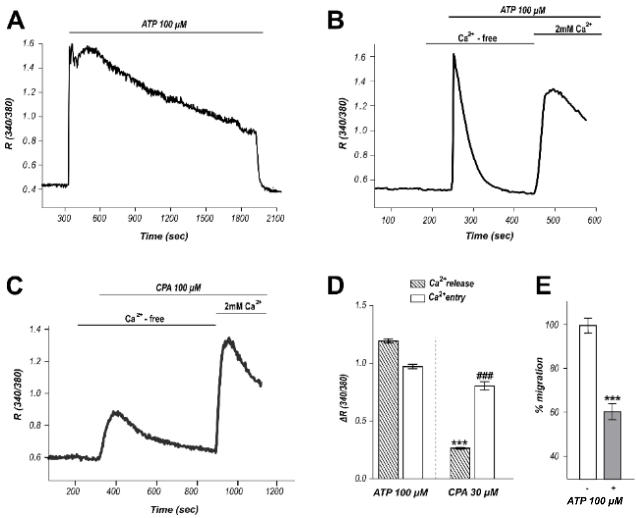

Figure 7. **Characterization of high ATP stimulation in RTEC.** (**A**) Representative tracing of Ca^{2+} signals evoked by 100 µM ATP in RTEC. (**B**) Representative tracing of the "Ca^{2+} add-back protocol upon 100 µM ATP. (**C**) Representative tracing of the "Ca^{2+} add-back protocol upon 30 µM CPA. (**D**) Quantification of Ca^{2+} release and Ca^{2+} entry evoked by 100 µM ATP and 30 µM CPA. Data are expressed as mean ± SEM. T-test: *** pValue < 0.0005 vs ATP Ca^{2+} release; Mann-Whitney test: ### pValue < 0.0005 vs ATP Ca^{2+} entry. (**E**) Representative wound healing experiment performed in RTEC. Data are expressed as percentage of migration at 8 hours. Data are normalized to the corresponding control and are expressed as mean ± SEM. T-test: *** pValue < 0.0005.

2. ATP-induced Calcium Release and Calcium Entry

In order to separate and quantify the two components of the ATP-evoked Ca^{2+} signals, i.e., the Ca^{2+} release from intracellular stores and Ca^{2+} entry from the extracellular medium, we applied the "Ca^{2+} add-back" protocol (see Materials and Methods) during the 100 μM ATP stimulation in BTECs (**Figure 8 A**). Cells were thus first stimulated with 100 μM ATP in 0 Ca^{2+}_{out} and only once $[Ca^{2+}]_c$ returned to the basal conditions, the extracellular Ca^{2+} was re-added. Following the 2 mM Ca^{2+} addition to the extracellular recording solution, in the continuous presence of the agonist, it was observed a sustained increase in the $[Ca^{2+}]_c$. This second $[Ca^{2+}]_c$ increase represents the extracellular Ca^{2+} entry due to the intracellular Ca^{2+} release, i.e., SOCE mechanisms induced by ATP stimulation. The expression of a functional SOCE machinery in BTECs was unveiled stimulating cells with 30 μM Cyclopiazonic acid (CPA) or 2 μM Thapsigargin (TG), two widely used ER depletors and thus SOCE activators (**Figure 8 B**), by using the Ca^{2+} add-back protocol.

Interesting, very similar results were obtained in RTECs (**Figure 7 B–D**): they activate SOCE machinery in response to 100 μM ATP stimulation.

3. SOCE is not required for the ATP-induced anti-migratory activity

Given the activation of SOCE machinery following ATP stimulation in BTECs, we employed a pharmacological approach to modulate the SOCE-related components of the Ca^{2+} response to 100 μM ATP and better clarify their contribution in the anti-migratory effect on BTECs previously reported[14].

First, we tested the Ca^{2+} response to 2 μM TG stimulation with the Ca^{2+} add-back protocol in presence of the SOCE inhibitor BTP-2. As expected, pre-treatment (20 minutes) with 20 μM BTP-2 completely abolished TG-induced Ca^{2+} entry in add-back experiments (**Figure 8 C**, **D**). We then repeated the same treatment with 20 μM BTP-2 in order to evaluate its effect of the ATP-induced Ca^{2+} entry: this experiment revealed that 20 μM BTP-2 inhibits ATP-mediated Ca^{2+} entry leaving unaltered the release from the internal stores but interestingly, a subpopulation of cells showed a significative BTP-2-insensitive component, suggesting the existence of a non-SOCE component (**Figure 8 E**, **F**) in the Ca^{2+} signal. This observation is in nice agreement with an expression of functional store-independent and Ca^{2+}-permeable P2XR-related ion channels, previously described in TEC[14]. The inhibition of $InsP_3Rs$ by 5

minutes pre-incubation with 100 μM 2-APB significantly reduced both ATP-induced Ca^{2+} entry and release (**Figure 8 E**, **F**).

To evaluate the potential involvement of ATP-induced Ca^{2+} release and Ca^{2+} entry component in BTECs migration, we performed migration assays treating cells with the pharmacological SOCE activators and inhibitors previously tested (**Figure 8 G**). First, we treated cells with 30 μM CPA or 2 μM TG or 100 μM 2-APB, and then we evaluated cells migration after 8 hours from the treatment, in presence and absence of 100 μM ATP. Either CPA, TG, and 2-APB alone, remarkably reduced BTECs migration compared to control (CTRL) condition. However, co-incubation with both ATP and CPA or TG or 2-APB produced further anti-migratory activity, showing that the ER-related component is not the only mechanism responsible for the functional effect. Subsequently, we repeated the same protocol treating cells with 20 μM BTP-2, in presence and absence of 100 μM ATP, and we observed that a complete inhibition of SOCE, by BTP-2 pre-incubation, failed to alter the ATP-mediated inhibitory effect on BTECs migration (**Figure 8 G**).

These results suggested that SOCE machinery does not play a major role in the ATP-mediated inhibitory effect on BTECs migration.

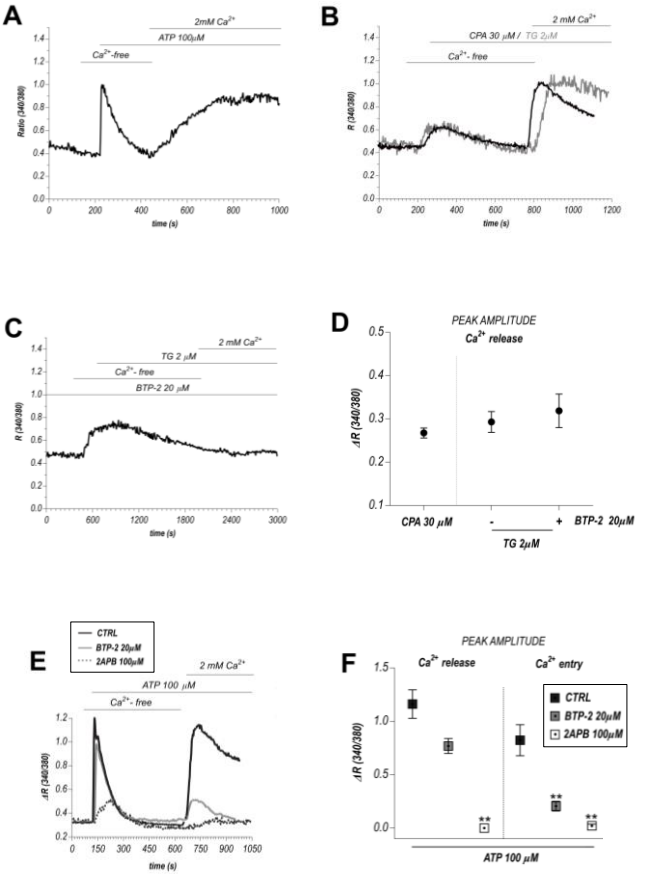
A
2mM Ca2+
ATP 100µM
Ca2+-free
Ratio (340/380)
time (s)
B
2 mM Ca2+
CPA 30 µM / TG 2µM
Ca2+- free
R (340/380)
time (s)
C
2 mM Ca2+
TG 2 µM
Ca2+- free
BTP-2 20 µM
R (340/380)
time (s)
D
PEAK AMPLITUDE
Ca2+ release
ΔR (340/380)
CPA 30 µM
-
+ BTP-2 20µM
TG 2µM
E
CTRL
BTP-2 20µM
2APB 100µM
2 mM Ca2+
ATP 100 µM
Ca2+- free
ΔR (340/380)
time (s)
F
PEAK AMPLITUDE
Ca2+ release
Ca2+ entry
CTRL
BTP-2 20µM
2APB 100µM
ΔR (340/380)
ATP 100 µM

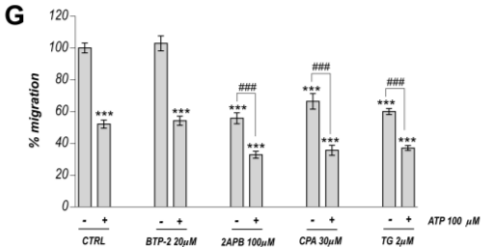

Figure 8. Ca^{2+} release, SOCE and relative involvement in anti-migratory action of high ATP. (**A**, **B**) Representative average traces obtained from the application of the "Ca^{2+} add-back" protocol upon treatment with 100 μM ATP (**A**), 30 μM CPA or 2 μM TG. (**C**) Preincubation with 20 μM BTP-2 (20 min) completely abolished TG-induced SOCE. Representative average trace. (**D**) Quantification of the previous experiments. Data are expressed as mean ± SEM. (**E**) Effect of preincubation with 20 μM BTP-2 or 100 μM 2-APB on ATP-induced calcium response. Representative average traces. (**F**) Quantification of the previous experiments. Data are expressed as mean SEM. ** p-value < 0.005 vs. CTRL. (**G**) BTECs migration evaluated by scratch wound healing measurements. Effects of CPA, TG, BTP-2, 2-APB. Data are expressed as percentage of migration at 8 h, normalized to the corresponding control (CTRL) and expressed as mean ± SEM. Mann-Whitney test: *** p-value < 0.0005 vs. CTRL; ### p-value < 0.0005.

4. Calcium Signals mediated by other Purinergic Agonists

Since we previously reported that the anti-migratory activity of ATP on BTECs is mimed by the other purinergic agonist ADP but not by UTP[14], we decided to extend our investigation about the purinergic-induced intracellular Ca^{2+} signals in BTECs to a wider purinergic stimulation, in order to find a correlation between the different functional effect and Ca^{2+} signals.

ADP and UTP were tested a three different concentration, i.e., 1, 10 and 100 μM, and both of them evoked a dose-response $[Ca^{2+}]_c$ increase in physiological extracellular solution (**Figure 9 A–F**). As previously for ATP, we adopted the Ca^{2+} add-back protocol to quantify Ca^{2+} release and Ca^{2+} entry triggered by 100 μM ADP or UTP (**Figure 9 G–I**). Despite the different functional responses following ADP or UTP treatment in BTECs, by using this experimental approach we did not detect any significative difference in Ca^{2+} responses.

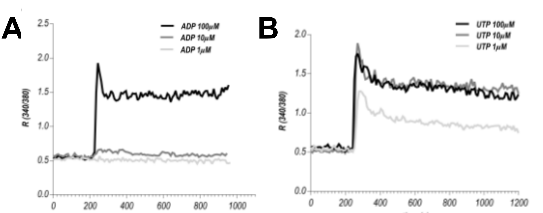

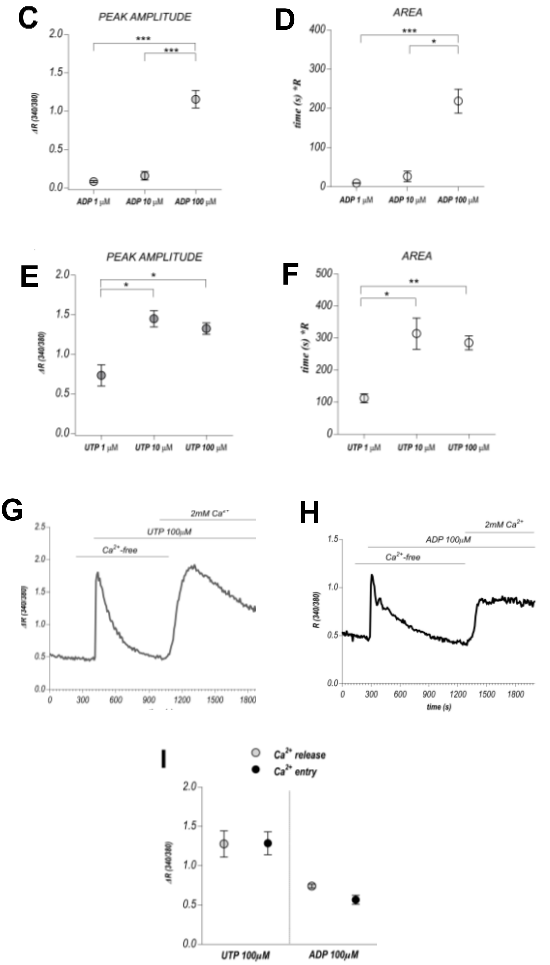
C
PEAK AMPLITUDE
ΔR (340/380)
ADP 1 μM
ADP 10 μM
ADP 100 μM
D
AREA
time (s) * R
E
PEAK AMPLITUDE
UTP 1 μM
UTP 10 μM
UTP 100 μM
F
AREA
G
2mM Ca2+
UTP 100μM
Ca2+-free
H
ADP 100μM
R (340/380)
time (s)
I
Ca2+ release
Ca2+ entry
UTP 100μM
ADP 100μM

Figure 9. High eADP and eUTP stimulation triggers biphasic Ca^{2+} signals in BTEC. Representative traces of different Ca^{2+} signals evoked by three different ADP (**A**) and UTP (**B**) concentrations (1, 10, 100 μM). (**C–D**) Quantification of the peak amplitude and area obtained upon 1, 10, 100 μM ADP stimulation. Area is calculated at 300 s from the beginning of the response. Data are expressed as mean ± SEM. * p-value < 0.05; ** p-value < 0.005 *** p-value < 0.0005. (**E–F**) The same quantifications of peak amplitude and area for eUTP stimulation. (**G–I**) Representative average traces obtained from the application of the Ca^{2+} add-back protocol upon treatment with 100 μM ADP or 100 μM UTP and relative quantifications. Data are expressed as mean ± SEM.

5. Contribution of Intracellular Organelles in the Purinergic-Induced Calcium Release

Considering that we did not detect any significative correlation between Ca^{2+} signals evoked by different purinergic agonists and the functional response, and that SOCE-component of ATP-induced Ca^{2+} signals is not involved in the inhibitory effect of BTECs migration, we decided to evaluate the contribution of different intracellular organelles (lysosomes, mitochondria and ER) to the Ca^{2+} response induced by purinergic stimulations. We hypothesized that a differential contribution could be responsible for the functional

effect could be masked by the quantification of the global intracellular Ca^{2+} release.

Therefore, we compared the Ca^{2+} store dynamics involved in the response to 100 μM ATP to the response to 100 μM UTP. A pharmacological approach was employed, based on the use of 2 μM TG (to deplete ER), 20 μM Bafilomycin A1 (Baf-A1, to affect lysosomes) and 1 μM FCCP (to uncouple mitochondria). All the experiments were performed in 0 Ca^{2+}_{out} by the use of two different protocols. First, we treated cells with the organelle-specific depletor and then, when $[Ca^{2+}]_c$ returned to basal conditions, we stimulated with 100 μM ATP or 100 μM UTP (**Figure 10 A–C**). Thus, by the quantification of the purinergic-induced Ca^{2+} response obtained following the depletion of one specific organelle, we evaluated the contribution of that Ca^{2+} store to the purinergic-induced Ca^{2+} response. Quantification included three parameters as major descriptors of Ca^{2+} release: peak amplitude, area and the decay tau of the Ca^{2+} spikes (**Figure 10 D–I**). Pretreatment with 20 μM Baf-A1 or 1 μM FCCP affected the features of both the spikes induced by ATP or UTP. Cells pretreated with TG drastically decreased the responses to ATP as well as to UTP, suggesting a major contribution for ER: however, a small TG-insensitive component could be detected, suggesting that other stores may be recruited by ATP and UTP.

Preincubation with the ionophore Ionomycin (Iono, 2 μM), that completely prevented Ca^{2+} response to ATP, was used as control condition. Moreover, the application of a second experimental protocol, based on a first stimulation with purinergic agonists and a second with Ca^{2+} stores depletors, confirmed the involvement of all three the examined organelles. In fact, there was a complete abolition of the $[Ca^{2+}]_c$ increase induced by TG, Baf-A1 or FCCP in cells pretreated with ATP or UTP (**Figure 10 J–L**), globally indicating an interplay among ER, mitochondria and lysosomes in the Ca^{2+} release triggered by both the purinergic agonists.

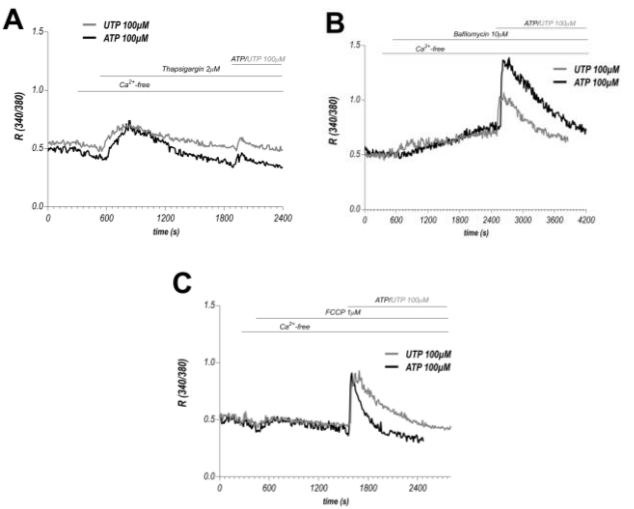

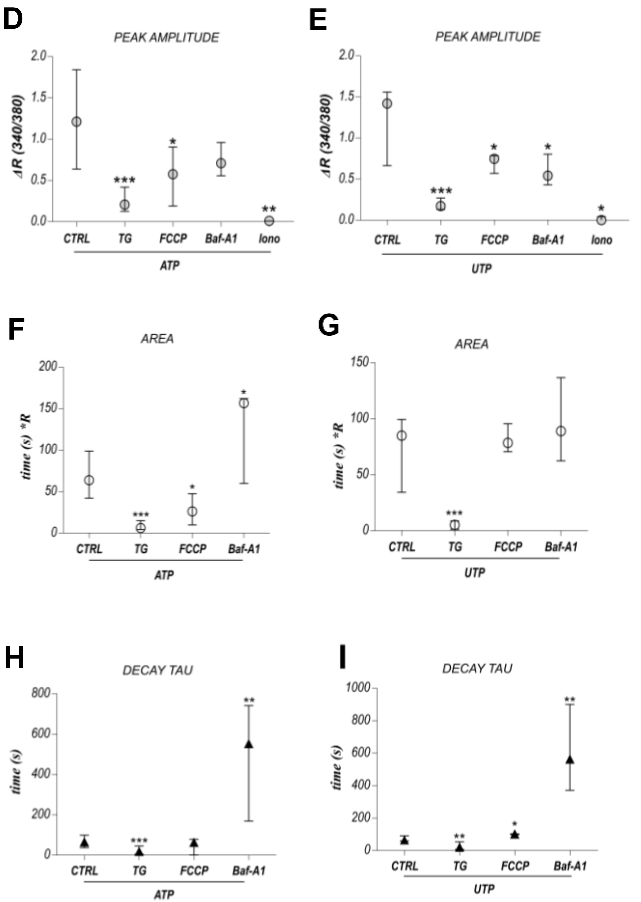
D
PEAK AMPLITUDE
ΔR (340/380)
2.0
1.5
1.0
0.5
0.0
***
*
**
CTRL
TG
FCCP
Baf-A1
Iono
ATP
E
PEAK AMPLITUDE
ΔR (340/380)
2.0
1.5
1.0
0.5
0.0
***
*
*
*
CTRL
TG
FCCP
Baf-A1
Iono
UTP
F
AREA
time (s) *R
200
150
100
50
0
***
*
*
CTRL
TG
FCCP
Baf-A1
ATP
G
AREA
time (s) *R
150
100
50
0
***
CTRL
TG
FCCP
Baf-A1
UTP
H
DECAY TAU
time (s)
800
600
400
200
0
***
**
CTRL
TG
FCCP
Baf-A1
ATP
I
DECAY TAU
time (s)
1000
800
600
400
200
0
**
**
*
CTRL
TG
FCCP
Baf-A1
UTP

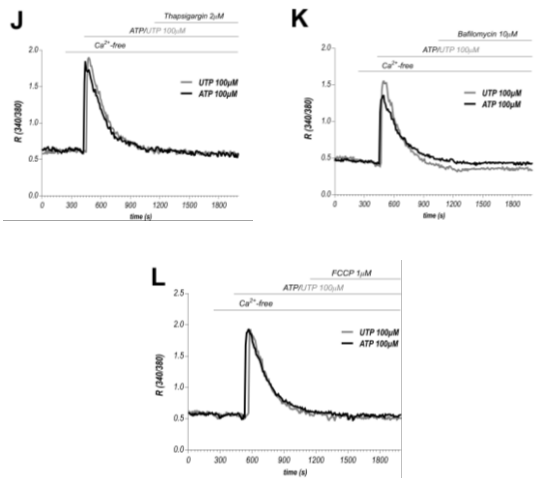

Figure 10. Interplay among different intracellular organelles in BTEC. (**A–C**) Effect of 2 μM TG, 10 μM Baf-A1 and 1 μM FCCP on the responses to 100 μM eATP or UTP. Representative traces. (**D–I**) Quantification of the previous experiments: peak amplitude, total area under the calcium spike and decay time. Data are expressed as median over the total range of values. * p-value < 0.05; ** p-value < 0.005; *** p-value < 0.0005 vs. CTRL. (**J–L**) Effect of TG, Baf-A1 and FCCP in cells pretreated with 100 μM ATP or UTP.

6. P2X7R-induced Calcium Signals

In the first part of the work, we focused on purinergic-evoked Ca^{2+} signals in BTECs in order to (I) define which components of the intracellular

Ca^{2+} signaling toolkit are activated upon purinergic agonists stimulation and (II) find a correlation between Ca^{2+} dynamics and differential functional effects among purinergic agonists. Since we found that intracellular organelles equally contribute to the ATP (potent inhibitor of BTECs migration) and UTP (agonist that failed to exert the anti-migratory activity in BTECs) intracellular Ca^{2+} release, and that SOCE-component of the ATP-induced Ca^{2+} signal is not required for the functional effect, we decided to focus on the non-SOCE component that still continue to operate extracellular Ca^{2+} entry in response to 100 μM ATP, even in the presence of SOCE inhibitor BTP-2. According to the literature, the non-SOCE component may be attributed to P2XRs activation and one of them, the P2X7R, was previously reported to be expressed in BTECs and its specific activation with the ATP analogue BzATP (100μM) was shown to mimic the inhibitory effect of ATP on BTECs migration[14].

We observed that 100μM BzATP application evoked a long lasting and sustained $[Ca^{2+}]_c$ increase in BTECs (**Figure 11 D–F**), strictly dependent on the presence of the agonist, as revealed by the rapid and reversible recovery to the resting Ca^{2+} levels upon agonist washout (**Figure 11 G**). Interestingly, stimulation of HMECs with 100μM BzATP (**Figure 11 D–F**), as well as 100μM ATP (**Figure 11 A–C**), revealed Ca^{2+} response in HMECs to be

minor than BTECs. The quantitative analysis of Ca^{2+} signals took into account the peak amplitude and area underlying the Ca^{2+} response (calculated within 300 seconds from the treatment). Moreover, the partial and reversible reduction of the Ca^{2+} signal upon acute treatment with the P2X7 antagonist BBG (**Figure 11 H**), unveiled that P2X7 activation is part of the 100 μM ATP-evoked Ca^{2+} response in BTECs.

Therefore, these results indicate a possible correlation between the activation of P2X7R in BTECs and the inhibitory effect on cells migration, that is lacking in HMECs displaying also quantitative minor Ca^{2+} response to 100 μM BzATP compared to BTECs.

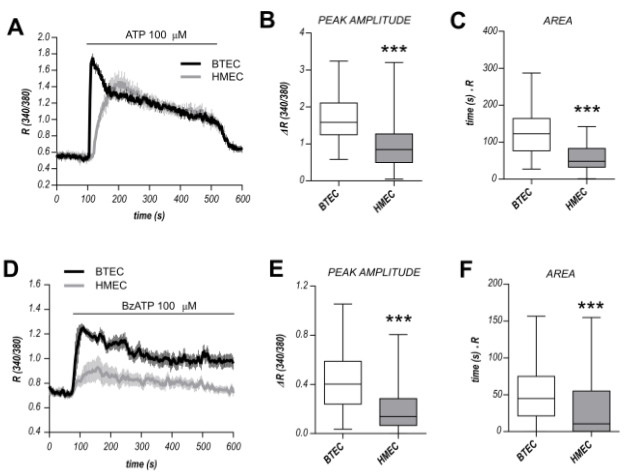

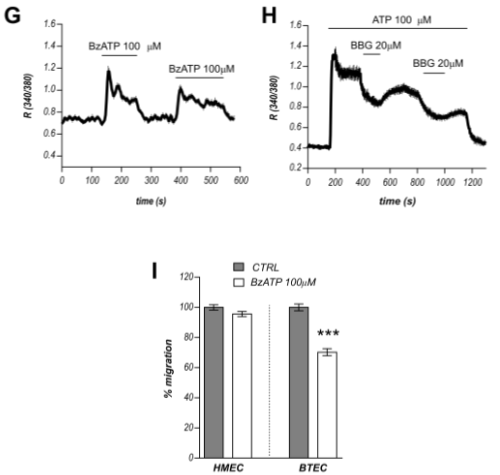

Figure 11. **Purinergic stimulation in BTECs include P2X7R activation.** (**A**) Representative average traces of 100 μM ATP stimulation in HMECs and BTECs. (**B**, **C**) Quantification of the peak amplitude and area obtained upon 100 μM ATP stimulation in HMECs and BTECs. Area is calculated at 300 s from the beginning of the response. Data are expressed as mean ± SEM. *** p-value < 0.0005. (**D**) Representative average traces of 100 μM BzATP stimulation in HMECs and BTECs. (**E**, **F**) Quantification of the peak amplitude and area obtained upon 100 μM ATP stimulation in HMECs and BTECs. Area is calculated at 300 s from the beginning of the response. Data are expressed as mean ± SEM. *** p-value < 0.0005. (**G**) Representative average traces of 100 μM BzATP stimulation and washout. (**H**) Representative average traces obtained from the application of 20 μM BBG in presence of 100 μM ATP treatment.

(**I**) BTECs and HMECs migration evaluated by scratch wound healing measurements. Effects of 100 μM BzATP. Data are
expressed as percentage of migration at 8 h, normalized to the corresponding control (CTRL) and expressed as mean ± SEM. Mann-Whitney test: *** p-value < 0.0005 vs CTRL.

7. P2X7R sensitivity to extracellular environment ions

Given the possible correlation between P2X7R activation and the functional response of BTECs following high purinergic stimulation with 100 μM ATP, next experiments were carried out in order to better investigated the P2X7R-induced Ca^{2+} response in BTECs.

Since the well know P2Xs family sensitivity to allosteric modulators such as cations and trace metals, we decide to modify the concentrations of different environmental ions (H^+, Zn^{2+}, Ca^{2+}) in the extracellular recording solutions and then evaluate the 100 μM BzATP-evoked Ca^{2+} response. Preincubation with extracellular 50 μM $ZnCl_2$, 10 mM $CaCl_2$ or with an acidic medium (pH 6.4) drastically reduced the $[Ca^{2+}]_c$ increase triggered by BzATP in BTECs (**Figure 12 A–F**). Interestingly, 10 μM $ZnCl_2$ was not able to inhibits BzATP-evoked Ca^{2+} signals in BTEC (**Figure 12 A**). These results, in accordance with the literature,

demonstrated that increased concentrations of extracellular Zn^{2+}, Ca^{2+} or H^{+} inhibit P2X7R pore activation.

Ultimately, we investigated the effects of extracellular Zn^{2+}, that showed a dose-dependent role in blocking pore channel activation, in the BzATP-induced anti-migratory effect on BTECs. We were not able to detect the functional effect of 100 μM BzATP in BTECs migration in the presence of 50 μM $ZnCl_2$ (**Figure 12 G**).

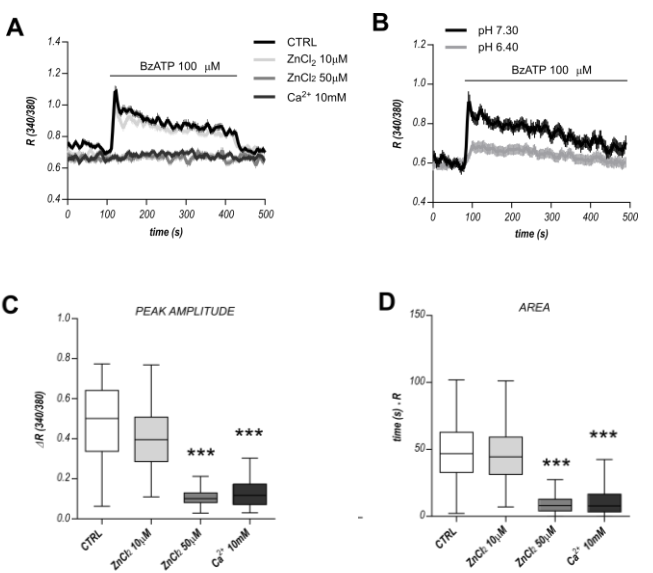

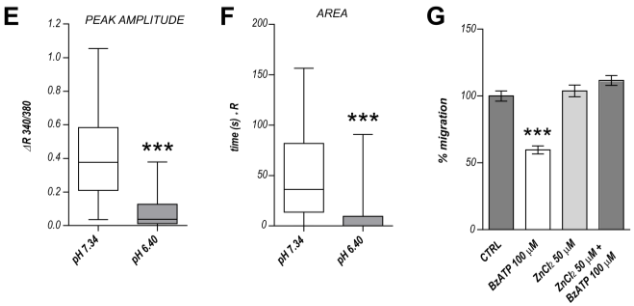

Figure 12. P2X7R-induced Ca^{2+} signals are modulated by environmental ions. (**A**) Representative average traces of 100 μM BzATP stimulation in BTECs, in presence of 50 μM $ZnCl_2$, 10 μM $ZnCl_2$ and 10 mM $CaCl_2$ in the extracellular solution. (**B**) Representative average traces of 100 μM BzATP stimulation in BTECs, in physiological (7.34) or acidic (6.4) extracellular pH. (**C**, **D**) Quantification of the peak amplitude and area obtained upon 100 μM BzATP stimulation in presence of 50 μM $ZnCl_2$, 10 μM $ZnCl_2$ and 10 mM $CaCl_2$ in the extracellular solution. Area is calculated at 300 s from the beginning of the response. Data are expressed as mean ± SEM. *** p-value < 0.0005. (**E**, **F**) Quantification of the peak amplitude and area obtained upon 100 μM BzATP stimulation in physiological (7.34) or acidic (6.4) extracellular pH. Area is calculated at 300 s from the beginning of the response. Data are expressed as mean ± SEM. *** p-value < 0.0005. (**G**) BTECs migration evaluated by scratch wound healing measurements. Effects of 100 μM BzATP in presence of 50 μM $ZnCl_2$. Data are expressed as percentage of migration at 8 h, normalized to the corresponding control (CTRL) and expressed as mean ± SEM. *** p-value < 0.0005 vs CTRL.

8. BzATP-mediated P2X7 activation inhibits TECs and not NECs migration

In the last part of the work we studied the role of BzATP-induced P2X7R activation in other two types of TECs: from renal (RTEC) and prostate (PTEC, characterized in[241]) cancer.

RTECs showed BzATP-evoked Ca^{2+} signals similar to BTECs in both peak amplitude and area quantification (**Figure 13 B**, **D**), on the contrary, PTECs didn't show any Ca^{2+} response to 100 μM BzATP stimulation (**Figure 13 B**).

We then move to the functional evaluation of BzATP stimulation in RTECs and PTECs migration: surprisingly, in both cases 100 μM BzATP still continued to inhibit cells migration (**Figure 13 A**). This result suggests the possibility of a Ca^{2+}-independent pathways responsible for the purinergic mediated anti-migratory effect on TECs.

Since these data indicate the possible activation of a P2X7R-induced and TEC-specific pathway, we decided to conditionate NECs (HMECs), previously showed quantitative less responsive to BzATP than BTECs, with a breast cancer cells line (MCF-7) for 72 hours. In this way we obtained NECs conditioned by the presence of cancer cells on which then evaluate, both the Ca^{2+} signals and the functional response to 100 μM BzATP treatment. Migration of HMECs co-coltured with

MCF7 (HMECs w/MCF7) resulted affected by 100 μM BzATP, showing an acquired sensitivity to the purinergic stimulation by HMECs, provided by the presence of MCF-7. In fact, BzATP reduced migration of HMECs w/MCF7 (**Figure 13 A**) while no effect was observed in the migration of our control condition represented by HMECs co-coltured for 72 hours with HMECs themselves. Moreover, quantitative analysis of 100 μM BzATP-induced Ca^{2+} signals is HMECs w/MCF7 did not show any significative differences with the control condition (HMECs) (**Figure 13 C**, **E**, **F**).

These data indicate that the BzATP-induced P2X7R activation leading the functional effect, is specific only for TECs and seems to be strictly dependent on the environmental conditions, i.e., the presence of cancer cells confers to NECs the sensitivity to the purinergic anti-migratory effect without altering the Ca^{2+} signals.

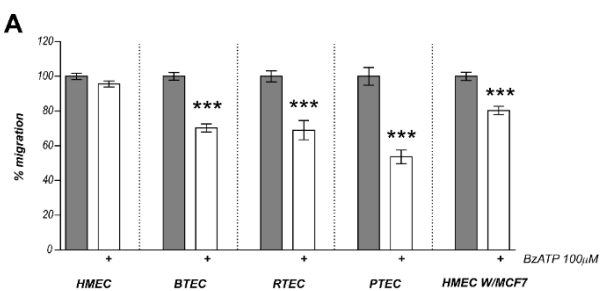

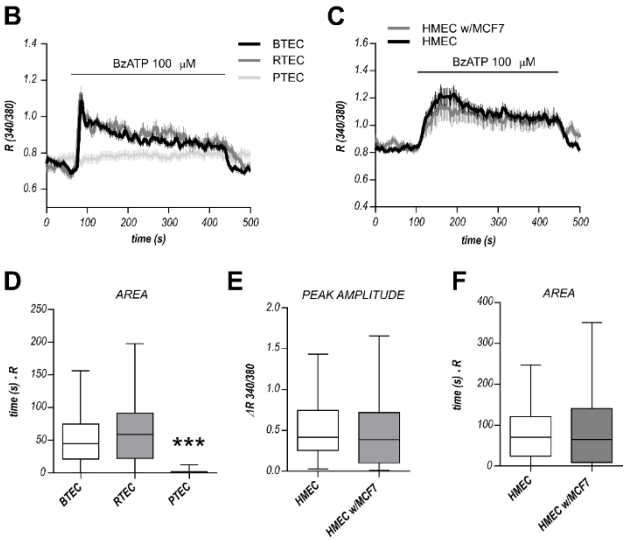

Figure 13. P2X7R activation mediates the inhibition of migration only in TECs. (**A**) BTECs migration evaluated by scratch wound healing measurements. Effects of 100 μM BzATP in HMECs, BTECs, RTECs, PTECs and HMEC w/MCF7. Data are expressed as percentage of migration at 8 h, normalized to the corresponding control (CTRL) and expressed as mean ± SEM. *** p-value < 0.0005 vs CTRL. (**B**) Representative average traces of 100 μM BzATP stimulation in BTECs, RTECs and PTECs. (**C**) Representative average traces of 100 μM BzATP stimulation in HMECs and HMECs w/MCF7. (**D**) Quantification of area obtained upon 100 μM BzATP stimulation in BTECs, RTECs and PTECs. (**E**, **F**) Quantification of peak amplitude and area obtained upon 100 μM BzATP stimulation in in HMECs and HMECs w/MCF7.

Discussion

Previous study showed that high non-physiological eATP doses (> 20 μM) strongly inhibit migration of ECs from human breast carcinoma (BTECs), while no effect on NECs (HMECs), and enhances *in vitro* endothelial normalization[14]. These events could be related to an overall potential anti-angiogenic and pro-normalizing activity of strong purinergic stimulation in cancer. Since eATP accumulation is gaining growing consensus as one the hallmarks of TME and that purinergic signaling have been deeply investigated in cancer cells, further investigations about its role on tumor endothelium, could be useful to enhance the comprehension of the mechanisms regulating one important step of tumor progression, i.e., tumor angiogenesis. In fact, few data are available about the role of purinergic stimulation in TECs.

In the first part of the work, we studied the purinergic-mediated Ca^{2+} signals in BTECs. We showed that different ATP concentrations (1, 10, 100 μM) evoke a dose-dependent intracellular Ca^{2+} increase shaped by a first transient peak followed by a sustained long-lasting phase. According to the literature, the observed ATP-evoked Ca^{2+} signals, both at high and low concentrations, are due to the intracellular Ca^{2+} release (probably the main actor

in the peak phase of the signal) and the extracellular Ca^{2+} influx (mainly related to the long-sustained phase of the signals) that was completely abolished after the removal of extracellular Ca^{2+}.

Then, we deeply focused on the 100 μM ATP-evoked Ca^{2+} signals because in accordance with the previous work, it is the unique, among the three tested concentrations, able to inhibit BTECs migration. Since both metabotropic P2Ys and ionotropic P2Xs receptor are widely and ubiquitously expressed by the cells, and members of these family were shown to be expressed by BTECs, we pointed out that the biphasic ATP-induced $[Ca^{2+}]_c$ increase is shaped in the initial transient $[Ca^{2+}]_c$ rise by the activation of both P2Ys and P2Xs, of which P2Ys mainly participate to the Ca^{2+} mobilization from intracellular stores. Regarding the long-lasting plateau phase of the signals, it is certainly due to the Ca^{2+} entry through the plasma membrane, e.g., is lacking in the experiments carried out in absence of extracellular Ca^{2+}, and is shaped by the recruitment of both P2Xs and SOCE machinery. SOCE, in fact, activates following ER Ca^{2+} content drop, as in this case following metabotropic P2Ys activation. We clearly observed the presence of functional SOCE machinery both in BTECs and RTECs when stimulated with 30 μM CPA or 2 μM TG, two widely used ER depletors. The pharmacological

inhibition of SOCE with 20 μM BTP-2 significantly prevented ATP-mediated Ca^{2+} entry in BTECs but did not completely abolish the plateau phase, revealing the non-SOCE component of Ca^{2+} entry induced by 100 μM ATP, reasonably related to P2X-ionotropic receptors activation.

Once highlighted the components of the intracellular Ca^{2+} signaling toolkit involved following 100 μM ATP in BTECs, we moved to study their involvement in the functional effect on BTECs migration. The ability of 100 μM ATP to decrease BTECs migration even in the presence of 20 μM BTP-2, unveiled a SOCE-independent component involvement in the anti-migratory effect of ATP. We analyzed the role of intracellular Ca^{2+} mobilization in BTECs migration and observed that the intracellular Ca^{2+} stores globally affect BTECs migration since the treatment with CPA or TG, two ER-calcium depletors, as well as 2-APB, remarkably impairs BTECs migration. This evidence points to a general involvement of ER-related Ca^{2+} release in the regulation of constitutive BTECs migration; nonetheless, and intriguingly, the ability of ATP to retain its anti-migratory activity even in TG-preconditioned cells indicates that at least a significant component of ATP-induced functional effects is independent of the release of Ca^{2+} from ER. The idea that Ca^{2+} stores could be necessary but not selectively required to

sustain the anti-migratory action of high eATP is further strengthened by the failure of 100 μM UTP, that actually triggers a Ca^{2+} release similar to that measured upon ATP stimulation, to promote the same functional effect of ATP. Moreover, a detailed quantitative pharmacological investigation by the use of drugs that selectively impair ER (2 μM TG), lysosomes (20 μM Baf-A1) and mitochondria (1 μM FCCP) led us to support an interplay among these intracellular organelles in the shaping of purinergic-related Ca^{2+} release in BTECs: however, no dramatic differences were detected in the quantitative features of this process comparing responses to ATP, that inhibits migration, and UTP, that fails to exert the same functional effect. The other purinergic agonist ADP, acting on P2Y-metabotropic receptors, is able to interfere with TECs migration [14] and elicit similar Ca^{2+} signals to ATP and UTP. Overall, these data suggest that SOCE and Ca^{2+} release from intracellular stores are not strictly and selectively required for the anti-migratory action of ATP on human tumoral endothelium, leading our interest to further investigations about the recruitment of P2X-ionotropic receptors that act as Ca^{2+}-permeable channels[3].

In the second part of the work, we mainly focused on P2X7R activation, that is the most prominent candidate among P2Xs family, widely

studied and often associated with over-expression in cancer cells[176,182,186]. Among P2Xs, P2X7R is preferentially activated by high eATP concentrations[143] and its expression was previously reported in BTECs[14]. According to the literature, the ATP analogue BzATP is at least one order of magnitude more potent than ATP at P2X7R, even if we cannot exclude also its considerable activity at other P2Xs isoforms[139,143]. Since 100 μM BzATP, mimed the effect of ATP by inhibiting only BTECs migration but not HMECs[14], we decided to analyze 100 μM BzATP-evoked Ca^{2+} signals in BTECs compared to those triggered in HMECs. The idea of a putative involvement of P2X7R activation in the purinergic-induced inhibition of BTECs migration was further strengthened by the quantitative lower BzATP-evoked intracellular Ca^{2+} mobilization in HMECs compared to BTECs. Moreover, P2X7R activation was confirmed to be part of the ATP-induced Ca^{2+} signals in BTECs by the partial and reversible reduction of the Ca^{2+} signal upon the acute treatment with a P2X7R antagonist 20 μM BBG (previously showed to partially rescue the inhibitory effect of ATP on BTECs migration[14]).

Given the possible involvement of P2X7R in the anti-migratory effect of purinergic stimulation in BTECs, we decided to deeper investigate the intracellular Ca^{2+} signaling induced by its activation.

Particularly, it is well known P2X7R sensitivity to different environmental cues typical in TME (e.g., acidosis, high eATP, cations) and the investigations about its activation and modulation in TECs represents a good opportunity to study the influence of certain tumor environmental characteristic on tumor vascularization. First, we decided to alter the extracellular concentrations of different ions (Zn^{2+}, H^+ and Ca^{2+}) and to evaluate the 100 μM BzATP-evoked Ca^{2+} response in BTECs. The presence of $ZnCl_2$ in the extracellular recording solution unveiled a dose-dependent modulation by Zn^{2+} of the BzATP-induced Ca^{2+} signals: only 50 μM $ZnCl_2$ completely abolished the Ca^{2+} signals while 10 μM $ZnCl_2$ didn't affect the Ca^{2+} response to BzATP. The presence of high Ca^{2+} (10mM $CaCl_2$) or H^+ (extracellular pH solution at 6.4) drastically reduced the $[Ca^{2+}]_c$ increase triggered by BzATP in BTECs, suggesting the inhibition of the pore channel. These results are in accordance with the well described in literature P2X7R allosteric modulations by cations, pH and trace metals[6]. Moreover, in the presence of 50 μM $ZnCl_2$ we did not observe any functional effect of BzATP in BTECs migration, suggesting that the intracellular pathway activated by purinergic stimulation and responsible for the anti-migratory activity in BTECs is sensible to the presence of extracellular Zn^{2+}.

Finally, we move to study the P2X7R-induced purinergic stimulation in other two TECs models: from renal (RTECs) and prostate (PTECs) cancer. RTECs, as previously reported for ATP[242], showed a 100 μM BzATP-induced Ca^{2+} response similar to BTECs. On the contrary, PTECs did not show any Ca^{2+} response to 100 μM BzATP treatment. Intriguingly, we observed that 100 μM BzATP, as well as in BTECs, inhibits migration of both RTECs and PTECs, even in the absence of intracellular Ca^{2+} mobilization following the receptor activation (PTECs). These data pointed out to a possible Ca^{2+}-independent pathway involvement in the purinergic-induced anti-migratory effect on TECs migration.

Ultimately, since no effect of 100μM BzATP was detected in HMECs migration, we decided to co-coltured HMECs for 72 hours with the breast cancer cells line MCF-7 and then to test the BzATP effect on their migration. Interestingly, the presence of MCF-7 appeared to confer BzATP sensitivity to HMECs: the conditioning with MCF-7 was sufficient to activate the BzATP-induced inhibitory effect also in HMECs migration.

Conclusion

Taking together my data suggest that purinergic stimulation activates a TEC-specific pathway that inhibits cells migration. This functional effect is mediated by the activation of P2X7-ionotropic receptors, plasma membrane Ca^{2+} channels usually over-expressed and associated with a pro-tumoral activity in cancer cells[176,195]. P2X7Rs activation in cancer cells, in fact, often leads to enhanced cell proliferation and migration through the activation of different intracellular signaling pathways such ERK 1/2 or PI3K/Akt[190,193,194].

In this work we showed that the functional effect of P2X7R activation in TECs is not correlated with the intracellular Ca^{2+} mobilization following the pore channel opening but is strictly influenced by the extracellular environment conditions. The presence of both organic (breast cancer cells) and inorganic elements (extracellular ions), in fact, alter the activation of the intracellular pathway responsible for the functional effect. Interestingly, the activation of ERK 1/2 intracellular pathway, often associated with P2X7R, was shown to occur in both Ca^{2+}-dependent or independent way[243] and, even more interesting, it is modulated by the presence of Zn^{2+} [244–246]. Since both of these characteristics associated with ERK 1/2 pathway emerged from the presented results,

we can speculate that the activation of P2X7R in TECs may passing through ERK 1/2 phosphorylation to exploit the anti-migratory activity.

Further investigations about the mechanisms involved in the P2X7R-mediated high purinergic stimulation-induced inhibition of TECs migration are certainly needed. Once identified them, it would be interesting to study their possible modulation by the typical TME cues (acidosis, hypoxia, increased ECM stiffness), to which P2X7R is particularly sensitive, in order to obtain more knowledge about the mechanisms that regulate tumor angiogenesis, considering the environmental conditions in which they take place.

Materials and Methods

1. Cell Cultures

Breast Tumor-derived ECs (BTECs), Renal Tumor-derived ECs (RTEC) and Prostate Tumor-derived ECs, respectively from human breast lobular-infiltrating carcinoma, renal and prostate carcinoma biopsy, were isolated and periodically characterized in the laboratory of Prof. Benedetta Bussolati (Department of Internal Medicine, Molecular Biotechnology Center and Research in Experimental Medicine Center, University of Torino, Italy).

Human Microvascular ECs (HMECs) are dermal-derived cells purchased from ATCC.

MCF-7 is human breast adenocarcinoma-derived cell line purchased from Sigma-Aldrich (Merck Millipore).

BTECs, RTECs, PTECs and HMECs were grown in EndoGRO-MV-VEGF Complete Media Kit composed of EndoGRO Basal Medium and EndoGRO-MV-VEGF Supplement Kit (Merck Millipore). EndoGRO Basal Medium is a low serum culture media for human microvascular ECs, supplemented with a kit containing rhVEGF (5 ng/mL), rhEGF (5 ng/mL), rhFGF (5 ng/mL), rhIGF-1 (15 ng/mL), L-Glutamine (10 mM),

Hydrocortisone Hemisuccinate (1.0 μg/mL), Heparin Sulfate (0.75 U/mL), Ascorbic Acid (50 μg/mL), Fetal Bovine Serum – FBS (5%).

MCF7 were grown in Dulbecco's Modified Eagle's Medium (DMEM) High Glucose (EuroClone®), supplemented with 10% FBS and 2% L-Glutamine.

All cell cultures were maintained in incubator (37°C and 5% CO_2 atmosphere), using Falcon® plates as supports (about 5000 cells/cm^2) and were used at passage 3 to 15.

HMECs were co-coltured with MCF-7 using Corning® Transwell® Permeable Supports for 6 well plate (24 mm diameter), with 0.4 μm pore polyester membrane, or with HMECs themselves as control condition. Cells were co-coltured in EndoGRO-MV-VEGF Complete Media Kit (previously described composition) and maintained in incubator (37°C and 5% CO_2 atmosphere) for 72 hours. HMECs were plate at the usual density of about 5000 cells/cm^2 while MCF-7 or HMECs for the conditioning were plate with 5-fold major cellular density. At the end of 72 hours, the co-colture was interrupted in order to plate HMECs according to the need of the experiment to be conducted.

2. Chemicals

ATP, ADP, UTP, BzATP, BTP2, Bafilomycin A-1, FCCP, Thapsigargin, Ionomycin, $ZnCl_2$ and $CaCl_2$ are purchased from Sigma-Aldrich (Merck); Fura-2AM and 2-APB are purchased from ThermoFisher.

Tyrode Standard was used extracellular physiological recording solution for Cell Calcium Imaging experiments. It is composed of 154 mM NaCl, 4 mM KCl, 2 mM $CaCl_2$, 1 mM $MgCl_2$, 5 mM HEPES, 5.5 mM Glucose (purchased from Sigma-Aldrich – Merck). Solution pH was adjusted to 7.4 using NaOH (purchased from Sigma-Aldrich – Merck). Cell Calcium Imaging experiments in extracellular Ca^{2+}-free conditions were carried out using a modified Tyrode Standard external solution, omitting the $CaCl_2$ salt from the formulation and adding the Ca^{2+} chelator EGTA (5 mM). Solution pH was adjusted to 7.4 and 6.4 using NaOH, for physiological and acidic condition, respectively.

3. Cell Calcium Imaging

Calcium Imaging experiments were carried out on cells grown on 32 mm diameter glass at a density of 5000 cells/cm^2 for 24-48 hours. Cells were next loaded with the fluorescent and ratiometric Ca^{2+}

indicator Fura-2AM (2 μM) for 30 minutes in incubator at 37 °C (37°C and 5% CO_2 atmosphere). Thus, the ratiometric cytosolic Ca^{2+} measurements (see also [234,236]) were performed keeping dark by using a set-up of Polychrome V spectrofluorimeter (TILL Photonics, Munich BioRegio, Germany) attached to a Nikon TE-2000-S (Nikon Corporation, Tokio, Japan) microscope. Metafluor Imaging System (Molecular Devices, Sunnyvale, CA, USA) was used for image acquisition using 3-second intervals. For each experiment, several regions of interest (ROIs) have been selected corresponding to cells in the chosen image field. Real time background subtraction was used in order to limit noise. The software records fluorescence intensities after excitation at the selected wavelengths.

Tyrode Standard was used as physiologic extracellular recording solution to maintain cells during the experiments, and as a solution for the treatments. For experiments in Ca^{2+}-free conditions, the external solution was modified omitting the $CaCl_2$ salt from the formulation and adding the Ca^{2+} chelator EGTA (see previous paragraph).

Ca^{2+} influx during the sustained phase was evaluated measuring the peak amplitude and area at 300 seconds after the onset of the agonist-response. We considered this time as it is sufficient so that the

Ca^{2+} store depletion is ended. Ca^{2+} store depletion and SOCE were evaluated by exploiting the "Ca^{2+} add-back" protocol: cells were treated with the agonist to induce depletion of Ca^{2+} stores in Ca^{2+}-free extracellular solution ($0Ca^{2+}{}_{out}$) and, subsequently, replaced with Ca^{2+}-containing solution (2 mM Ca^{2+}) so that SOCE could be measured. Ca^{2+} store depletion and SOCE were quantified evaluating the peak amplitude of the responses.

4. Migration Assay

Culture-insert assay were performed to evaluate cells migration: cells were plated in EndoGRO-MV-VEGF Complete Media Kit (previously described composition) on 12-well culture plates using silicone culture inserts (purchased from IBIDI GmbH, Planegg, Germany). Each insert had three 70 μL chambers, used to plate cells ($3\text{-}5 \cdot 10^5$ cells/mL density). Cells were maintained in incubator until confluence within the chambers was reached. Cell monolayers were starved 2 hours in EndoGRO-MV Media Kit, without FBS and without VEGF, and only after the inserts were be removed. Cells were then washed with PBS solution and treatments were added in duplicate. EndoGRO-MV 5% FBS without VEGF was used as positive control.

Experiments were performed using a Nikon Eclipse Ti (Nikon Corporation, Tokio, Japan) inverted microscope equipped with a A.S.I. MS-2000 stage and a OkoLab incubator (to keep cells at 37°C and 5% CO_2). Images were acquired at 2h time intervals using a Nikon Plan 4X/0.10 objective and a CCD camera. MetaMorph software (Molecular Devices, Sunnyvale, CA, USA) was used to acquire images for 5 time points (8 hours).

5. Data Analysis and Statistics

Calcium imaging analysis and quantification (peak amplitude, area, decay time) were performed using Clampfit software (Axon PClamp, Molecular Devices, San Jose, CA, USA) and analyzed with GraphPad Prism 7 (GraphPad Software, Inc., La Jolla, CA, USA). Area underlying Ca^{2+} influx during the sustained phase in the presence of extracellular Ca^{2+} was evaluated at 300 seconds after the onset of the response. Total area under Ca^{2+} spikes in 0 Ca^{2+}_{out} was measured by the use of Event Detection protocol in Clampfit software. Each ROI was analyzed in order to determine $[Ca^{2+}]_c$ increase and to calculate the parameters of Ca^{2+} responses.

Wound healing experiments with inserts were analyzed using Metamorph software. Cell migration was assessed by measuring the distance between the

two sides of the wound at each time point. Obtained data were further analyzed using Excel in order to calculate the percentage of migration for each wound (difference of distances between cell fronts at two subsequent time points over distance at time = 0 hours) and the percentage mean value for each condition was then calculated. At least six fields for each condition were analyzed in each independent experiment.

Statistical analysis of all experiments was performed using GraphPad Prism 7 (GraphPad Software, Inc., La Jolla, CA, USA). Each experiment was repeated at least three times. Preliminary Shapiro-Wilk test was performed to check the normal distributions of each dataset: accordingly, statistical analysis was performed by using either the non-parametric Mann-Whitney test or the Student's t-test. A p-Value of < 0.05 was considered significant.

Bibliography

1. Mittal, K., Ebos, J. & Rini, B. Angiogenesis and the tumor microenvironment: Vascular endothelial growth factor and beyond. *Semin. Oncol.* **41**, 235–251 (2014).
2. Pellegatti, P. *et al.* Increased level of extracellular ATP at tumor sites: In vivo imaging with plasma membrane luciferase. *PLoS One* **3**, e2599 (2008).
3. Burnstock, G. & Di Virgilio, F. Purinergic signalling and cancer. *Purinergic Signal.* **9**, 491–540 (2013).
4. Burnstock, G. Purine and purinergic receptors. *Brain Neurosci. Adv.* **2**, 2398212818817494 (2018).
5. Virginio, C., Church, D., North, R. A. & Surprenant, A. Effects of divalent cations, protons and calmidazolium at the rat P2X7 receptor. *Neuropharmacology* **36**, 1285–1294 (1997).
6. Coddou, C., Stojilkovic, S. S. & Huidobro-Toro, J. P. Allosteric modulation of ATP-gated P2X receptor channels. *Rev. Neurosci.* **22**, 335–354 (2011).
7. Liu, X., Ma, W., Surprenant, A. & Jiang, L.-H. Identification of the amino acid residues in the extracellular domain of rat P2X(7) receptor involved in functional inhibition by

acidic pH. *Br. J. Pharmacol.* **156**, 135–42 (2009).
8. Acuña-Castillo, C., Coddou, C., Bull, P., Brito, J. & Huidobro-Toro, J. P. Differential role of extracellular histidines in copper, zinc, magnesium and proton modulation of the P2X7 purinergic receptor. *J. Neurochem.* **101**, 17–26 (2007).
9. Azimi, I. *et al.* Altered purinergic receptor-Ca2+ signaling associated with hypoxia-induced epithelial-mesenchymal transition in breast cancer cells. *Mol. Oncol.* **10**, 166–178 (2016).
10. Tafani, M. *et al.* Hypoxia-increased RAGE and P2X7R expression regulates tumor cell invasion through phosphorylation of Erk1/2 and Akt and nuclear translocation of NF-κB. *Carcinogenesis* **32**, 1167–1175 (2011).
11. Hope, J. M., Greenlee, J. D. & King, M. R. Mechanosensitive Ion Channels: TRPV4 and P2X7 in Disseminating Cancer Cells. *Cancer J. (United States)* **24**, 84–92 (2018).
12. Pethő, Z., Najder, K., Bulk, E. & Schwab, A. Mechanosensitive ion channels push cancer progression. *Cell Calcium* **80**, 79–90 (2019).
13. Vultaggio-Poma, V., Sarti, A. C. & Di Virgilio, F. Extracellular ATP: A Feasible Target for Cancer Therapy. *Cells* **9**, (2020).
14. Avanzato, D. *et al.* Activation of P2X7 and

P2Y11 purinergic receptors inhibits migration and normalizes tumor-derived endothelial cells via cAMP signaling. *Sci. Rep.* **6**, (2016).

15. Anderson, N. M. & Simon, M. C. The tumor microenvironment. *Curr. Biol.* **30**, R921–R925 (2020).
16. Ansell, S. M. & Vonderheide, R. H. Cellular Composition of the Tumor Microenvironment. *Am. Soc. Clin. Oncol. Educ. B.* **33**, e91–e97 (2013).
17. Hanahan, D. & Weinberg, R. A. The Hallmarks of Cancer Review evolve progressively from normalcy via a series of pre. *Cell* **100**, 57–70 (2000).
18. Hanahan, D. & Coussens, L. M. Accessories to the crime: functions of cells recruited to the tumor microenvironment. *Cancer Cell* **21**, 309–322 (2012).
19. Arneth, B. Tumor microenvironment. *Medicina (B. Aires).* **56**, 15 (2020).
20. Jain, R. K. Normalization of Tumor Vasculature: An Emerging Concept in Antiangiogenic Therapy. *Science (80-.).* **307**, 58–62 (2005).
21. Carmeliet, P. & Jain, R. K. Principles and mechanisms of vessel normalization for cancer and other angiogenic diseases. *Nat. Rev. Drug Discov.* **10**, 417–427 (2011).

22. Scarpellino, G., Munaron, L., Cantelmo, A. R. & Fiorio Pla, A. Calcium-Permeable Channels in Tumor Vascularization: Peculiar Sensors of Microenvironmental Chemical and Physical Cues. *Rev. Physiol. Biochem. Pharmacol.* (2020) doi:10.1007/112_2020_32.
23. Ayob, A. Z. & Ramasamy, T. S. Cancer stem cells as key drivers of tumour progression. *J. Biomed. Sci.* **25**, 20 (2018).
24. Coussens, L. M. & Werb, Z. Inflammation and cancer. *Nature* **420**, 860–867 (2002).
25. Grivennikov, S. I., Greten, F. R. & Karin, M. Immunity, Inflammation, and Cancer. *Cell* **140**, 883–899 (2010).
26. Shieh, Y. S. *et al.* Tumor-associated macrophage correlated with angiogenesis and progression of mucoepidermoid carcinoma of salivary glands. *Ann. Surg. Oncol.* **16**, 751–760 (2009).
27. Lamagna, C., Aurrand-Lions, M. & Imhof, B. A. Dual role of macrophages in tumor growth and angiogenesis. *J. Leukoc. Biol.* **80**, 705–713 (2006).
28. Riabov, V. *et al.* Role of tumor associated macrophages in tumor angiogenesis and lymphangiogenesis. *Front. Physiol.* **5**, 75 (2014).
29. Valković, T. *et al.* Correlation between vascular endothelial growth factor,

angiogenesis, and tumor-associated macrophages in invasive ductal breast carcinoma. *Virchows Arch.* **440**, 583–588 (2002).
30. Alkasalias, T., Moyano-Galceran, L., Arsenian-Henriksson, M. & Lehti, K. Fibroblasts in the tumor microenvironment: Shield or spear? *Int. J. Mol. Sci.* **19**, 1532 (2018).
31. Truffi, M., Sorrentino, L. & Corsi, F. Fibroblasts in the Tumor Microenvironment. *Adv. Exp. Med. Biol.* **1234**, 15–29 (2020).
32. Fiori, M. E. *et al.* Cancer-associated fibroblasts as abettors of tumor progression at the crossroads of EMT and therapy resistance. *Mol. Cancer* **18**, (2019).
33. Sobierajska, K., Ciszewski, W. M., Sacewicz-Hofman, I. & Niewiarowska, J. Endothelial Cells in the Tumor Microenvironment. *Adv. Exp. Med. Biol.* **1234**, 71–86 (2020).
34. Chen, L., Endler, A. & Shibasaki, F. Hypoxia and angiogenesis: Regulation of hypoxia-inducible factors via novel binding factors. *Exp. Mol. Med.* **41**, 849–857 (2009).
35. Hanahan, D. & Weinberg, R. A. Hallmarks of cancer: The next generation. *Cell* **144**, 646–674 (2011).
36. Dudley, A. C. Tumor endothelial cells. *Cold*

Spring Harb. Perspect. Med. **2**, (2012).
37. Bussolati, B., Deambrosis, I., Russo, S., Deregibus, M. C. & Camussi, G. Altered angiogenesis and survival in human tumor-derived endothelial cells. *FASEB J.* **17**, 1159–1161 (2003).
38. Hida, K. *et al.* Tumor-associated endothelial cells with cytogenetic abnormalities. *Cancer Res.* **64**, 8249–8255 (2004).
39. Grange, C. *et al.* Isolation and characterization of human breast tumor-derived endothelial cells. *Oncol. Rep.* **15**, 381–386 (2006).
40. De Palma, M., Biziato, D. & Petrova, T. V. Microenvironmental regulation of tumour angiogenesis. *Nat. Rev. Cancer* **17**, 457–474 (2017).
41. Padera, T. P. *et al.* Cancer cells compress intratumour vessels. *Nature* **427**, 695 (2004).
42. Di Tomaso, E. *et al.* Mosaic tumor vessels: Cellular basis and ultrastructure of focal regions lacking endothelial cell markers. *Cancer Res.* **65**, 5740–5749 (2005).
43. De Val, S. & Black, B. L. Transcriptional Control of Endothelial Cell Development. *Dev. Cell* **16**, 180–195 (2009).
44. Maniotis, A. J. *et al.* Vascular channel formation by human melanoma cells in vivo and in vitro: Vasculogenic mimicry. *Am. J.*

Pathol. **155**, 739–752 (1999).
45. McDonald, D. M., Munn, L. & Jain, R. K. Vasculogenic mimicry: How convincing, how novel, and how significant? *Am. J. Pathol.* **156**, 383–388 (2000).
46. St. Croix, B. *et al.* Genes expressed in human tumor endothelium. *Science (80-.).* **289**, 1197–1202 (2000).
47. Lugano, R., Ramachandran, M. & Dimberg, A. Tumor angiogenesis: causes, consequences, challenges and opportunities. *Cell. Mol. Life Sci.* **77**, 1745–1770 (2020).
48. Potente, M., Gerhardt, H. & Carmeliet, P. Basic and therapeutic aspects of angiogenesis. *Cell* **146**, 873–887 (2011).
49. Scott, A. M., Allison, J. P. & Wolchok, J. D. Monoclonal antibodies in cancer therapy. *Cancer Immun.* **12**, 14 (2012).
50. Pottier, C. *et al.* Tyrosine kinase inhibitors in cancer: Breakthrough and challenges of targeted therapy. *Cancers (Basel).* **12**, (2020).
51. Munaron, L., Genova, T., Avanzato, D., Antoniotti, S. & Fiorio Pla, A. Targeting Calcium Channels to Block Tumor Vascularization. *Recent Pat. Anticancer. Drug Discov.* **8**, 27–37 (2012).
52. Bussolati, B., Grange, C. & Camussi, G. Tumor exploits alternative strategies to achieve vascularization. *FASEB J.* **25**, 2874–

2882 (2011).
53. Moccia, F. *et al.* Endothelial progenitor cells support tumour growth and metastatisation: implications for the resistance to anti-angiogenic therapy. *Tumor Biol.* **36**, 6603–6614 (2015).
54. Zhu, H. *et al.* The mobilization, recruitment and contribution of bone marrow-derived endothelial progenitor cells to the tumor neovascularization occur at an early stage and throughout the entire process of hepatocellular carcinoma growth. *Oncol. Rep.* **28**, 1217–24 (2012).
55. Carmeliet, P. & Jain, R. Angiogenesis in cancer and other diseases. *Nature* **407**, 249–257 (2000).
56. Hillen, F. & Griffioen, A. W. Tumour vascularization: Sprouting angiogenesis and beyond. *Cancer Metastasis Rev.* **26**, 489–502 (2007).
57. Seano, G. & Jain, R. K. Vessel co-option in glioblastoma: emerging insights and opportunities. *Angiogenesis* **23**, 9–16 (2020).
58. Kunkel, P. *et al.* Inhibition of glioma angiogenesis and growth in Vivo by systemic treatment with a monoclonal antibody against vascular endothelial growth factor receptor-2. *Cancer Res.* **61**, 6624–6628 (2001).
59. Shen, Y. *et al.* Tumor vasculogenic mimicry

formation as an unfavorable prognostic indicator in patients with breast cancer. *Oncotarget* **8**, 56408–56416 (2017).
60. Lv, J. *et al.* Significance of Vasculogenic Mimicry Formation in Gastric Carcinoma. *Oncol. Res. Treat.* **40**, 35–41 (2017).
61. Zhuo, M. *et al.* JQ1 effectively inhibits vasculogenic mimicry of pancreatic ductal adenocarcinoma cells via the ERK1/2-MMP-2/9 signaling pathway both in vitro and in vivo. *Am. J. Transl. Res.* **11**, 1030–1039 (2019).
62. Poltavets, V., Kochetkova, M., Pitson, S. M. & Samuel, M. S. The Role of the Extracellular Matrix and Its Molecular and Cellular Regulators in Cancer Cell Plasticity. *Front. Oncol.* **8**, 431 (2018).
63. Zanotelli, M. R. & Reinhart-King, C. A. Mechanical forces in tumor angiogenesis. *Adv. Exp. Med. Biol.* **1092**, 91–112 (2018).
64. Mammoto, A. *et al.* A mechanosensitive transcriptional mechanism that controls angiogenesis. *Nature* **457**, 1103–1108 (2009).
65. Karki, P. & Birukova, A. A. Substrate stiffness-dependent exacerbation of endothelial permeability and inflammation: mechanisms and potential implications in ALI and PH (2017 Grover Conference Series). *Pulm. Circ.* **8**, 1–9 (2018).

66. Bordeleau, F. *et al.* Matrix stiffening promotes a tumor vasculature phenotype. *Proc. Natl. Acad. Sci. U. S. A.* **114**, 492–497 (2017).
67. Petrova, V., Annicchiarico-Petruzzelli, M., Melino, G. & Amelio, I. The hypoxic tumour microenvironment. *Oncogenesis* **7**, (2018).
68. Peitzsch, C., Perrin, R., Hill, R. P., Dubrovska, A. & Kurth, I. Hypoxia as a biomarker for radioresistant cancer stem cells. *Int. J. Radiat. Biol.* **90**, 636–652 (2014).
69. Boareto, M., Jolly, M. K., Ben-Jacob, E. & Onuchic, J. N. Jagged mediates differences in normal and tumor angiogenesis by affecting tip-stalk fate decision. *Proc. Natl. Acad. Sci. U. S. A.* **112**, E3836–E3844 (2015).
70. Lim To, W. K., Kumar, P. & Marshall, J. M. Hypoxia is an effective stimulus for vesicular release of ATP from human umbilical vein endothelial cells. *Placenta* **36**, 759–766 (2015).
71. Eubank, T. D., Roda, J. M., Liu, H., O'Neil, T. & Marsh, C. B. Opposing roles for HIF-1α and HIF-2α in the regulation of angiogenesis by mononuclear phagocytes. *Blood* **117**, 323–332 (2011).
72. Roda, J. M. *et al.* Stabilization of HIF-2α Induces sVEGFR-1 Production from Tumor-Associated Macrophages and

Decreases Tumor Growth in a Murine Melanoma Model. *J. Immunol.* **189**, 3168–3177 (2012).
73. Poletto, V. *et al.* The role of endothelial colony forming cells in kidney cancer's pathogenesis, and in resistance to anti-VEGFR agents and mTOR inhibitors: A speculative review. *Crit. Rev. Oncol. Hematol.* **132**, 89–99 (2018).
74. Barar, J. & Omidi, Y. Dysregulated pH in tumor microenvironment checkmates cancer therapy. *BioImpacts* **3**, 149–162 (2013).
75. Gonzalez, C. D. *et al.* Autophagy, Warburg, and Warburg Reverse Effects in Human Cancer. *Biomed Res. Int.* **2014**, 1–10 (2014).
76. Cardone, R. a, Casavola, V. & Reshkin, S. J. The role of disturbed pH dynamics and the NA+/H+ exchanger in metastasis. *Nat. Rev. Cancer* **5**, 786–795 (2005).
77. J. Reshkin, S., A. Cardone, R. & Harguindey, S. Na+-H+ Exchanger, pH Regulation and Cancer. *Recent Pat. Anticancer. Drug Discov.* **8**, 85–99 (2012).
78. Bourguignon, L. Y. W., Singleton, P. A., Diedrich, F., Stern, R. & Gilad, E. CD44 interaction with Na+-H+ exchanger (NHE1) creates acidic microenvironments leading to hyaluronidase-2 and cathepsin B activation and breast tumor cell invasion. *J.*

Biol. Chem. **279**, 26991–7007 (2004).
79. Dong, L. *et al.* Acidosis Activation of the Proton-Sensing GPR4 Receptor Stimulates Vascular Endothelial Cell Inflammatory Responses Revealed by Transcriptome Analysis. *PLoS One* **8**, 61991 (2013).
80. Asai, M. *et al.* Extracellular acidosis suppresses endothelial function by inhibiting store-operated Ca2+ entry via non-selective cation channels. *Cardiovasc. Res.* **83**, 97–105 (2009).
81. Di Virgilio, F. Purines, purinergic receptors, and cancer. *Cancer Res.* **72**, 5441–5447 (2012).
82. Burnstock, G. & Novak, I. Purinergic signalling in the pancreas in health and disease. *J. Endocrinol.* **213**, 123–141 (2012).
83. Burnstock, G. Pathophysiology and therapeutic potential of purinergic signaling. *Pharmacol. Rev.* **58**, 58–86 (2006).
84. Deli, T. & Csernoch, L. Extracellular ATP and cancer - An overview with special reference to P2 purinergic receptors. *Pathol. Oncol. Res.* **14**, 219–231 (2008).
85. Yegutkin, G. G. Nucleotide- and nucleoside-converting ectoenzymes: Important modulators of purinergic signalling cascade. *Biochim. Biophys. Acta - Mol. Cell Res.* **1783**, 673–694 (2008).

86. Burnstock, G. Purinergic signalling: Its unpopular beginning, its acceptance and its exciting future. *BioEssays* **34**, 218–225 (2012).
87. Erlinge, D. & Burnstock, G. P2 receptors in cardiovascular regulation and disease. *Purinergic Signal.* **4**, 1–20 (2008).
88. Burnstock, G. Purinergic regulation of vascular tone and remodelling. *Auton. Autacoid Pharmacol.* **29**, 63–72 (2009).
89. Antonioli, L., Yegutkin, G. G., Pacher, P., Blandizzi, C. & Haskó, G. Anti-CD73 in Cancer Immunotherapy: Awakening New Opportunities. *Trends in Cancer* **2**, 95–109 (2016).
90. Ferrari, D. *et al.* Purinergic signaling in scarring. *FASEB J.* **30**, 3–12 (2016).
91. Mello, P. de A., Coutinho-Silva, R. & Savio, L. E. B. Multifaceted effects of extracellular adenosine triphosphate and adenosine in the tumor-host interaction and therapeutic perspectives. *Front. Immunol.* **8**, 1526 (2017).
92. Burnstock, G. P2X ion channel receptors and inflammation. *Purinergic Signal.* **12**, 59–67 (2016).
93. Racine, M. L., Dinenno, F. A., Hogan, M. & Santana, F. Reduced deformability contributes to impaired deoxygenation-induced ATP release from red blood cells of

older adult humans. *Authors. J. Physiol. C* **597**, 4503–4519 (2019).
94. Milo, R., Jorgensen, P., Moran, U., Weber, G. & Springer, M. BioNumbers—the database of key numbers in molecular and cell biology. *Nucleic Acids Res.* **38**, (2010).
95. Lazarowski, E. R. Vesicular and conductive mechanisms of nucleotide release. *Purinergic Signal.* **8**, 359–373 (2012).
96. Di Virgilio, F., Dal Ben, D., Sarti, A. C., Giuliani, A. L. & Falzoni, S. The P2X7 Receptor in Infection and Inflammation. *Immunity* **47**, 15–31 (2017).
97. Oviedo-Orta, E. & Evans, W. H. Gap junctions and connexin-mediated communication in the immune system. *Biochim. Biophys. Acta - Biomembr.* **1662**, 102–112 (2004).
98. Adamson, S. E. & Leitinger, N. The role of pannexin1 in the induction and resolution of inflammation. *FEBS Lett.* **588**, 1416–1422 (2014).
99. Locovei, S., Wang, J. & Dahl, G. Activation of pannexin 1 channels by ATP through P2Y receptors and by cytoplasmic calcium. *FEBS Lett.* **580**, 239–244 (2006).
100. Qiu, F. & Dahl, G. A permeant regulating its permeation pore: Inhibition of pannexin 1 channels by ATP. *Am. J. Physiol. - Cell Physiol.*

296, C250 (2009).
101. Abbracchio, M. P. *et al.* International Union of Pharmacology LVIII: Update on the P2Y G protein-coupled nucleotide receptors: From molecular mechanisms and pathophysiology to therapy. *Pharmacol. Rev.* **58**, 281–341 (2006).
102. Abbracchio, M. P. *et al.* Characterization of the UDP-glucose receptor (re-named here the P2Y 14 receptor) adds diversity to the P2Y receptor family. *Trends Pharmacol. Sci.* **24**, 52–55 (2003).
103. Leo Bours, M. J., Dagnelie, P. C., Giuliani, A. L., Wesselius, A. & Di Virgilio, F. P2 receptors and extracellular ATP: A novel homeostatic pathway in inflammation. *Front. Biosci. - Sch.* **3 S**, 1443–1456 (2011).
104. Khakh, B. S. & Alan North, R. P2X receptors as cell-surface ATP sensors in health and disease. *Nature* **442**, 527–532 (2006).
105. Wirkner, K., Sperlagh, B. & Illes, P. P2X3 receptor involvement in pain states. *Mol. Neurobiol.* **36**, 165–183 (2007).
106. Zhuo, M., Wu, G. & Wu, L. J. Neuronal and microglial mechanisms of neuropathic pain. *Mol. Brain* **4**, 1–12 (2011).
107. Khakh, B. S. & North, R. A. Neuromodulation by Extracellular ATP and

P2X Receptors in the CNS. *Neuron* **76**, 51–69 (2012).
108. Kinnamon, S. C. & Finger, T. E. A taste for ATP: Neurotransmission in taste buds. *Front. Cell. Neurosci.* **7**, 264 (2013).
109. Idzko, M., Ferrari, D. & Eltzschig, H. K. Nucleotide signalling during inflammation. *Nature* **509**, 310–317 (2014).
110. Antonioli, L., Blandizzi, C., Pacher, P. & Haskó, G. Immunity, inflammation and cancer: A leading role for adenosine. *Nat. Rev. Cancer* **13**, 842–857 (2013).
111. Scarpellino, G., Genova, T. & Munaron, L. Purinergic P2X7 Receptor: A Cation Channel Sensitive to Tumor Microenvironment. *Recent Pat. Anticancer. Drug Discov.* **14**, 32–38 (2019).
112. Rapaport, E. Mechanisms of anticancer activities of adenine nucleotides in tumor-bearing hosts. *Ann. N. Y. Acad. Sci.* **603**, 142–9; discussion 149-50 (1990).
113. Feng, L. L., Cai, Y. Q., Zhu, M. C., Xing, L. J. & Wang, X. The yin and yang functions of extracellular ATP and adenosine in tumor immunity. *Cancer Cell Int.* **20**, 1–11 (2020).
114. Burnstock, G. Purinergic signaling and vascular cell proliferation and death. *Arterioscler. Thromb. Vasc. Biol.* **22**, 364–373 (2002).

115. Burnstock, G. Purinergic signalling: Therapeutic developments. *Front. Pharmacol.* **8**, (2017).
116. Strassheim, D. *et al.* P2Y Purinergic Receptors, Endothelial Dysfunction, and Cardiovascular Diseases. *Int. J. Mol. Sci.* **21**, 1–21 (2020).
117. Ralevic, V. P2X receptors in the cardiovascular system. *Wiley Interdiscip. Rev. Membr. Transp. Signal.* **1**, 663–674 (2012).
118. Yamamoto, K., Korenaga, R., Kamiya, A. & Ando, J. Fluid shear stress activates Ca2+ influx into human endothelial cells via P2X4 purinoceptors. *Circ. Res.* **87**, 385–391 (2000).
119. Loesch, A. & Burnstock, G. Ultrastructural localisation of ATP-gated P2X2 receptor immunoreactivity in vascular endothelial cells in rat brain. *Endothel. J. Endothel. Cell Res.* **7**, 93–98 (2000).
120. Hansen, M. A., Dutton, J. L., Balcar, V. J., Barden, J. A. & Bennett, M. R. P(2X) (purinergic) receptor distributions in rat blood vessels. *J. Auton. Nerv. Syst.* **75**, 147–155 (1999).
121. Meininger, C. J., Schelling, M. E. & Granger, H. J. Adenosine and hypoxia stimulate proliferation and migration of endothelial cells. *Am. J. Physiol. - Hear. Circ. Physiol.* **255**, (1988).

122. Van Daele, P., Van Coevorden, A., Roger, P. P. & Boeynaems, J. M. Effects of adenine nucleotides on the proliferation of aortic endothelial cells. *Circ. Res.* **70**, 82–90 (1992).
123. Cha, S. H., Hahn, T. W., Sekine, T., Lee, K. H. & Endou, H. Purinoceptor-mediated calcium mobilization and cellular proliferation in cultured bovine corneal endothelial cells. *Jpn. J. Pharmacol.* **82**, 181–187 (2000).
124. Gessi, S., Merighi, S., Sacchetto, V., Simioni, C. & Borea, P. A. Adenosine receptors and cancer. *Biochim. Biophys. Acta* **1808**, 1400–12 (2011).
125. Baldwin, J. M. Structure and function of receptors coupled to G proteins. *Curr. Opin. Cell Biol.* **6**, 180–190 (1994).
126. Schöneberg, T., Schulz, A. & Gudermann, T. The structural basis of G-protein-coupled receptor function and dysfunction in human diseases. *Rev. Physiol. Biochem. Pharmacol.* **144**, 143–227 (2002).
127. Fredholm, B. B., IJzerman, A. P., Jacobson, K. A., Linden, J. & Müller, C. E. International union of basic and clinical pharmacology. LXXXI. Nomenclature and classification of adenosine receptors - An update. *Pharmacol. Rev.* **63**, 1–34 (2011).
128. Sheth, S., Brito, R., Mukherjea, D., Rybak, L.

P. & Ramkumar, V. Adenosine receptors: Expression, function and regulation. *Int. J. Mol. Sci.* **15**, 2024–2052 (2014).
129. Klaasse, E. C., IJzerman, A. P., de Grip, W. J. & Beukers, M. W. Internalization and desensitization of adenosine receptors. *Purinergic Signal.* **4**, 21–37 (2008).
130. Erb, L. & Weisman, G. A. Coupling of P2Y receptors to G proteins and other signaling pathways. *Wiley Interdiscip. Rev. Membr. Transp. Signal.* **1**, 789–803 (2012).
131. Velázquez, B., Garrad, R. C., Weisman, G. A. & González, F. A. Differential agonist-induced desensitization of P2Y2 nucleotide receptors by ATP and UTP. *Mol. Cell. Biochem.* **206**, 75–89 (2000).
132. Köles, L. *et al.* Interaction of P2 purinergic receptors with cellular macromolecules. *Naunyn. Schmiedebergs. Arch. Pharmacol.* **377**, 1–33 (2008).
133. Volonté, C., Amadio, S., D'Ambrosi, N., Colpi, M. & Burnstock, G. P2 receptor web: Complexity and fine-tuning. *Pharmacol. Ther.* **112**, 264–280 (2006).
134. Erb, L., Liao, Z., Seye, C. I. & Weisman, G. A. P2 receptors: Intracellular signaling. *Pflugers Arch. Eur. J. Physiol.* **452**, 552–562 (2006).
135. North, R. A. P2X receptors. *Philos. Trans. R.*

Soc. B Biol. Sci. **371**, 20150427 (2016).
136. North, R. A. Molecular physiology of P2X receptors. *Physiol. Rev.* **82**, 1013–1067 (2002).
137. Saul, A., Hausmann, R., Kless, A. & Nicke, A. Heteromeric assembly of P2X subunits. *Front. Cell. Neurosci.* **7**, 250 (2013).
138. Alves, L. A. *et al.* Structural and molecular modeling features of P2X receptors. *Int. J. Mol. Sci.* **15**, 4531–4549 (2014).
139. North, R. A. & Jarvis, M. F. P2X receptors as drug targets. *Mol. Pharmacol.* **83**, 759–769 (2013).
140. Kaczmarek-Hájek, K., Lörinczi, É., Hausmann, R. & Nicke, A. Molecular and functional properties of P2X receptors-recent progress and persisting challenges. *Purinergic Signal.* **8**, 375–417 (2012).
141. Robinson, L. E. & Murrell-Lagnado, R. D. The trafficking and targeting of P2X receptors. *Front. Cell. Neurosci.* **7**, 233 (2013).
142. Anderson, C. M. & Nedergaard, M. Emerging challenges of assigning P2X7 receptor function and immunoreactivity in neurons. *Trends Neurosci.* **29**, 257–262 (2006).
143. Syed, N. i. H. & Kennedy, C. Pharmacology of P2X receptors. *Wiley Interdiscip. Rev. Membr. Transp. Signal.* **1**, 16–30 (2012).
144. Nicke, A., Kerschensteiner, D. & Soto, F. Biochemical and functional evidence for

heteromeric assembly of P2X1 and P2X4 subunits. *J. Neurochem.* **92**, 925–933 (2005).
145. Jiang, L. H. *et al.* Subunit arrangement in P2X receptors. *J. Neurosci.* **23**, 8903–8910 (2003).
146. Coddou, C., Yan, Z., Obsil, T., Huidobro-Toro, J. P. & Stojilkovic, S. S. Activation and Regulation of Purinergic P2X Receptor Channels. *Pharmacol. Rev.* **63**, 641–683 (2011).
147. Rettinger, J. *et al.* Profiling at recombinant homomeric and heteromeric rat P2X receptors identifies the suramin analogue NF449 as a highly potent P2X1 receptor antagonist. *Neuropharmacology* **48**, 461–468 (2005).
148. Aschrafi, A., Sadtler, S., Niculescu, C., Rettinger, J. & Schmalzing, G. Trimeric architecture of homomeric P2X2 and heteromeric P2X 1+2 receptor subtypes. *J. Mol. Biol.* **342**, 333–343 (2004).
149. Surprenant, A., Schneider, D. A., Wilson, H. L., Galligan, J. J. & North, R. A. Functional properties of heteromeric P2X(1/5) receptors expressed in HEK cells and excitatory junction potentials in guinea-pig submucosal arterioles. *J. Auton. Nerv. Syst.* **81**, 249–263 (2000).
150. Wildman, S. S. *et al.* Sensitization by

extracellular Ca2+ of rat P2X5 receptor and its pharmacological properties compared with rat P2X1. *Mol. Pharmacol.* **62**, 957–966 (2002).

151. Hausmann, R., Kless, A. & Schmalzing, G. Key Sites for P2X Receptor Function and Multimerization: Overview of Mutagenesis Studies on a Structural Basis. *Curr. Med. Chem.* **22**, 799–818 (2014).
152. Hattori, M. & Gouaux, E. Molecular mechanism of ATP binding and ion channel activation in P2X receptors. *Nature* **485**, 207–212 (2012).
153. Marquez-Klaka, B., Rettinger, J., Bhargava, Y., Eisele, T. & Nicke, A. Identification of an intersubunit cross-link between substituted cysteine residues located in the putative ATP binding site of the P2X1 receptor. *J. Neurosci.* **27**, 1456–66 (2007).
154. Ennion, S. J. & Evans, R. J. Conserved cysteine residues in the extracellular loop of the human P2X1 receptor form disulfide bonds and are involved in receptor trafficking to the cell surface. *Mol. Pharmacol.* **61**, 303–311 (2002).
155. Brown, S. G., Townsend-Nicholson, A., Jacobson, K. A., Burnstock, G. & King, B. F. Heteromultimeric P2X1/2 receptors show a novel sensitivity to extracellular pH.

J. Pharmacol. Exp. Ther. **300**, 673–680 (2002).
156. King, B. F. *et al.* Coexpression of rat P2X2 and P2X6 subunits in Xenopus oocytes. *J. Neurosci.* **20**, 4871–4877 (2000).
157. Tittle, R. K. & Hume, R. I. Opposite effects of zinc on human and rat P2X2 receptors. *J. Neurosci.* **28**, 11131–11140 (2008).
158. Nagaya, N., Tittle, R. K., Saar, N., Dellal, S. S. & Hume, R. I. An intersubunit zinc binding site in rat P2X2 receptors. *J. Biol. Chem.* **280**, 25982–25993 (2005).
159. Lorca, R. A. *et al.* Extracellular histidine residues identify common structural determinants in the copper/zinc P2X2 receptor modulation. *J. Neurochem.* **95**, 499–512 (2005).
160. Moore, S. F. & MacKenzie, A. B. Species and agonist dependent zinc modulation of endogenous and recombinant ATP-gated P2X7 receptors. *Biochem. Pharmacol.* **76**, 1740–1747 (2008).
161. Yan, Z., Khadra, A., Sherman, A. & Stojilkovic, S. S. Calcium-dependent block of P2X7 receptor channel function is allosteric. *J. Gen. Physiol.* **138**, 437–452 (2011).
162. Klapperstück, M., Büttner, C., Schmalzing, G. & Markwardt, F. Functional evidence of distinct ATP activation sites at the human

P2X7 receptor. *J. Physiol.* **534**, 25–35 (2001).
163. Li, M., Silberberg, S. D. & Swartz, K. J. Subtype-specific control of P2X receptor channel signaling by ATP and Mg2+. *Proc. Natl. Acad. Sci. U. S. A.* **110**, E3455–E3463 (2013).
164. Ikeda, T. Pharmacological effects of ivermectin, an antiparasitic agent for intestinal strongyloidiasis: Its mode of action and clinical efficacy. *Folia Pharmacol. Jpn.* **122**, 527–538 (2003).
165. Lê, K. T., Babinski, K. & Séguéla, P. Central P2X4 and P2X6 channel subunits coassemble into a novel heteromeric ATP receptor. *J. Neurosci.* **18**, 7152–9 (1998).
166. Khakh, B. S., Proctor, W. R., Dunwiddie, T. V, Labarca, C. & Lester, H. A. Allosteric control of gating and kinetics at P2X(4) receptor channels. *J. Neurosci.* **19**, 7289–99 (1999).
167. Priel, A. & Silberberg, S. D. Mechanism of Ivermectin Facilitation of Human P2X4 Receptor Channels. *J. Gen. Physiol.* **123**, 281–293 (2004).
168. Emmett, D. S. *et al.* Characterization of ionotrophic purinergic receptors in hepatocytes. *Hepatology* **47**, 698–705 (2008).
169. Nagaoka, M. *et al.* Regulation of adenosine 5'-triphosphate (ATP)-gated P2X4 receptors

on tracheal smooth muscle cells. *Respir. Physiol. Neurobiol.* **166**, 61–67 (2009).
170. Sim, J. A., Park, C. K., Oh, S. B., Evans, R. J. & North, R. A. P2X 1 and P2X 4 receptor currents in mouse macrophages. *Br. J. Pharmacol.* **152**, 1283–1290 (2007).
171. Wareham, K., Vial, C., Wykes, R. C. E., Bradding, P. & Seward, E. P. Functional evidence for the expression of P2X1, P2X4 and P2X7 receptors in human lung mast cells. *Br. J. Pharmacol.* **157**, 1215–1224 (2009).
172. Zemkova, H. *et al.* Characterization of purinergic P2X4 receptor channels expressed in anterior pituitary cells. *Am. J. Physiol. - Endocrinol. Metab.* **298**, (2010).
173. Nörenberg, W. *et al.* Positive allosteric modulation by ivermectin of human but not murine P2X7 receptors. *Br. J. Pharmacol.* **167**, 48–66 (2012).
174. Rokic, M. B. & Stojilkovic, S. S. Two open states of P2X receptor channels. *Front. Hum. Neurosci.* **7**, (2013).
175. Mehta, N. *et al.* Purinergic receptor P2X7: A novel target for anti-inflammatory therapy. *Bioorganic Med. Chem.* **22**, 54–88 (2014).
176. Young, C. N. J. & Górecki, D. C. P2RX7 purinoceptor as a therapeutic target-The second coming? *Front. Chem.* **6**, 248 (2018).
177. Burnstock, G. & Knight, G. E. The potential

of P2X7 receptors as a therapeutic target, including inflammation and tumour progression. *Purinergic Signal.* **14**, (2018).
178. Young, C. N. J. *et al.* A novel mechanism of autophagic cell death in dystrophic muscle regulated by P2RX7 receptor large-pore formation and HSP90. *Autophagy* **11**, 113–130 (2015).
179. Di Virgilio, F., Schmalzing, G. & Markwardt, F. The Elusive P2X7 Macropore. *Trends Cell Biol.* **28**, 392–404 (2018).
180. Kawano, A. *et al.* Involvement of P2X4 receptor in P2X7 receptor-dependent cell death of mouse macrophages. *Biochem. Biophys. Res. Commun.* **419**, 374–380 (2012).
181. Compan, V. *et al.* P2X2 and P2X5 subunits define a new heteromeric receptor with P2X7-like properties. *J. Neurosci.* **32**, 4284–4296 (2012).
182. A. Barden, J. Non-Functional P2X7: A Novel and Ubiquitous Target in Human Cancer. *J. Clin. Cell. Immunol.* **05**, (2014).
183. Gilbert, S. *et al.* ATP in the tumour microenvironment drives expression of nfP2X7, a key mediator of cancer cell survival. *Oncogene* **38**, 194–208 (2019).
184. Pan, H. *et al.* P2RX7-V3 is a novel oncogene that promotes tumorigenesis in uveal melanoma. *Tumor Biol.* **37**, 13533–13543

(2016).
185. Yang, Y. C. *et al.* Functional variant of the P2X7 receptor gene is associated with human papillomavirus-16 positive cervical squamous cell carcinoma. *Oncotarget* **7**, 82798–82803 (2016).
186. Adinolfi, E. *et al.* Accelerated tumor progression in mice lacking the ATP receptor P2X7. *Cancer Res.* **75**, 635–644 (2015).
187. Zhang, W. jun, Hu, C. gui, Zhu, Z. ming & Luo, H. liang. Effect of P2X7 receptor on tumorigenesis and its pharmacological properties. *Biomed. Pharmacother.* **125**, (2020).
188. Fang, J. *et al.* The expression of P2X7 receptors in EPCs and their potential role in the targeting of EPCs to brain gliomas. *Cancer Biol. Ther.* **16**, 498–510 (2015).
189. Hill, L. M., Gavala, M. L., Lenertz, L. Y. & Bertics, P. J. Extracellular ATP May Contribute to Tissue Repair by Rapidly Stimulating Purinergic Receptor X7-Dependent Vascular Endothelial Growth Factor Release from Primary Human Monocytes. *J. Immunol.* **185**, 3028–3034 (2010).
190. Ji, Z. *et al.* Involvement of P2X7 Receptor in Proliferation and Migration of Human Glioma Cells. *Biomed Res. Int.* **2018**, (2018).

191. Park, M. *et al.* Involvement of the P2X7 receptor in the migration and metastasis of tamoxifen-resistant breast cancer: effects on small extracellular vesicles production. *Sci. Rep.* **9**, 1–14 (2019).
192. Giannuzzo, A., Pedersen, S. F. & Novak, I. The P2X7 receptor regulates cell survival, migration and invasion of pancreatic ductal adenocarcinoma cells. *Mol. Cancer* **14**, (2015).
193. Xia, J., Yu, X., Tang, L., Li, G. & He, T. P2X7 receptor stimulates breast cancer cell invasion and migration via the AKT pathway. *Oncol. Rep.* **34**, 103–110 (2015).
194. Qiu, Y. *et al.* P2X7 Mediates ATP-Driven Invasiveness in Prostate Cancer Cells. *PLoS One* **9**, e114371 (2014).
195. Choi, J. H., Ji, Y. G., Ko, J. J., Cho, H. J. & Lee, D. H. Activating P2X7 Receptors Increases Proliferation of Human Pancreatic Cancer Cells via ERK1/2 and JNK. *Pancreas* **47**, 643–651 (2018).
196. Dewhirst, M. W., Lee, C. T. & Ashcraft, K. A. The future of biology in driving the field of hyperthermia. *Int. J. Hyperth.* **32**, 4–13 (2016).
197. Hirayama, Y. *et al.* Astrocyte-mediated ischemic tolerance. *J. Neurosci.* **35**, 3794–3805 (2015).
198. Hirayama, Y. & Koizumi, S. Hypoxia-

independent mechanisms of HIF-1α expression in astrocytes after ischemic preconditioning. *Glia* **65**, 523–530 (2017).
199. Amoroso, F. *et al.* The P2X7 receptor is a key modulator of the PI3K/GSK3β/VEGF signaling network: Evidence in experimental neuroblastoma. *Oncogene* **34**, 5240–5251 (2015).
200. Locovei, S., Scemes, E., Qiu, F., Spray, D. C. & Dahl, G. Pannexin1 is part of the pore forming unit of the P2X7 receptor death complex. *FEBS Lett.* **581**, 483–488 (2007).
201. Barden, J. A. Non-Functional P2X7: A Novel and Ubiquitous Target in Human Cancer. *J. Clin. Cell. Immunol.* **05**, (2014).
202. Young, C. N. J. *et al.* Sustained activation of P2X7 induces MMP-2-evoked cleavage and functional purinoceptor inhibition. *J. Mol. Cell Biol.* **10**, 229–242 (2018).
203. Berridge, M. J., Lipp, P. & Bootman, M. D. The versatility and universality of calcium signalling. *Nat. Rev. Mol. Cell Biol.* **1**, 11–21 (2000).
204. Thillaiappan, N. B., Chakraborty, P., Hasan, G. & Taylor, C. W. IP 3 receptors and Ca 2+ entry. *Biochim. Biophys. Acta - Mol. Cell Res.* **1866**, 1092–1100 (2019).
205. Raqeeb, A., Sheng, J., Ao, N. & Braun, A. P. Purinergic P2Y2 receptors mediate rapid

Ca2+ mobilization, membrane hyperpolarization and nitric oxide production in human vascular endothelial cells. *Cell Calcium* **49**, 240–248 (2011).

206. Lyubchenko, T. *et al.* P2Y1 and P2Y13 purinergic receptors mediate Ca2+ signaling and proliferative responses in pulmonary artery vasa vasorum endothelial cells. *Am. J. Physiol. - Cell Physiol.* **300**, (2011).
207. Jardin, I. & Rosado, J. A. STIM and calcium channel complexes in cancer. *Biochim. Biophys. Acta - Mol. Cell Res.* **1863**, 1418–1426 (2016).
208. Prakriya, M. & Lewis, R. S. Store-operated calcium channels. *Physiol. Rev.* **95**, 1383–1436 (2015).
209. Moccia, F. *et al.* Targeting Stim and Orai Proteins as an Alternative Approach in Anticancer Therapy. *Curr. Med. Chem.* **23**, 3450–3480 (2016).
210. Vashisht, A., Trebak, M. & Motiani, R. K. STIM and orai proteins as novel targets for cancer therapy. A review in the theme: Cell and molecular processes in cancer metastasis. *Am. J. Physiol. - Cell Physiol.* **309**, C457–C469 (2015).
211. Zuccolo, E. *et al.* Stim and Orai mediate constitutive Ca2+ entry and control endoplasmic reticulum Ca2+ refilling in

primary cultures of colorectal carcinoma cells. *Oncotarget* **9**, 31098–31119 (2018).
212. Pérez-Riesgo, E. *et al.* Transcriptomic Analysis of Calcium Remodeling in Colorectal Cancer. *Int. J. Mol. Sci.* **18**, 922 (2017).
213. Rhee, S. G. Regulation of phosphoinositide-specific phospholipase C. *Annu. Rev. Biochem.* **70**, 281–312 (2001).
214. Hisatsune, C., Nakamura, K., Kuroda, Y., Nakamura, T. & Mikoshiba, K. Amplification of Ca2+ signaling by diacylglycerol-mediated inositol 1,4,5-trisphosphate production. *J. Biol. Chem.* **280**, 11723–11730 (2005).
215. Glaser, T., Resende, R. R. & Ulrich, H. Implications of purinergic receptor-mediated intracellular calcium transients in neural differentiation. *Cell Commun. Signal.* **11**, 12 (2013).
216. Moccia, F. *et al.* P2Y1 and P2Y2 receptor-operated Ca2+ signals in primary cultures of cardiac microvascular endothelial cells. *Microvasc. Res.* **61**, 240–252 (2001).
217. Prevarskaya, N., Skryma, R. & Shuba, Y. Calcium in tumour metastasis: New roles for known actors. *Nat. Rev. Cancer* **11**, 609–618 (2011).
218. Tsai, F. C. & Meyer, T. Ca2+ pulses control

local cycles of lamellipodia retraction and adhesion along the front of migrating cells. *Curr. Biol.* **22**, 837–842 (2012).
219. Evans, J. H. & Falke, J. J. Ca2+ influx is an essential component of the positive-feedback loop that maintains leading-edge structure and activity in macrophages. *Proc. Natl. Acad. Sci. U. S. A.* **104**, 16176–16181 (2007).
220. Wei, C. *et al.* Calcium flickers steer cell migration. *Nature* **457**, 901–905 (2009).
221. Ridley, A. J. *et al.* Cell Migration: Integrating Signals from Front to Back. *Science (80-.).* **302**, 1704–1709 (2003).
222. Blaser, H. *et al.* Migration of Zebrafish Primordial Germ Cells: A Role for Myosin Contraction and Cytoplasmic Flow. *Dev. Cell* **11**, 613–627 (2006).
223. Cortesio, C. L., Boateng, L. R., Piazza, T. M., Bennin, D. A. & Huttenlocher, A. Calpain-mediated proteolysis of paxillin negatively regulates focal adhesion dynamics and cell migration. *J. Biol. Chem.* **286**, 9998–10006 (2011).
224. Franco, S. J. & Huttenlocher, A. Regulating cell migration: Calpains make the cut. *J. Cell Sci.* **118**, 3829–3838 (2005).
225. Munaron, L. & Pla, A. Endothelial Calcium Machinery and Angiogenesis:

Understanding Physiology to Interfere with Pathology. *Curr. Med. Chem.* **16**, 4691–4703 (2009).
226. Moccia, F. Update on vascular endothelial Ca 2+ signalling: A tale of ion channels, pumps and transporters. *World J. Biol. Chem.* **3**, 127 (2012).
227. Moccia, F. *et al.* Hematopoietic Progenitor and Stem Cells Circulate by Surfing on Intracellular Ca2+ Waves: A Novel Target for Cell-based Therapy and Anti-cancer Treatment? *Curr. Signal Transduct. Ther.* **7**, 161–176 (2012).
228. Dragoni, S. *et al.* Vascular endothelial growth factor stimulates endothelial colony forming cells proliferation and tubulogenesis by inducing oscillations in intracellular Ca 2+ concentration. *Stem Cells* **29**, 1898–1907 (2011).
229. Dragoni, S. *et al.* Canonical transient receptor potential 3 channel triggers vascular endothelial growth factor-induced intracellular Ca2+ oscillations in endothelial progenitor cells isolated from umbilical cord blood. *Stem Cells Dev.* **22**, 2561–2580 (2013).
230. Moccia, F. *et al.* Ca2+ Signalling in Endothelial Progenitor Cells: A Novel Means to Improve Cell-Based Therapy and Impair Tumour Vascularisation. *Curr. Vasc.*

Pharmacol. **12**, 87–105 (2014).
231. Lodola, F. *et al.* VEGF-induced intracellular Ca2+ oscillations are down-regulated and do not stimulate angiogenesis in breast cancer-derived endothelial colony forming cells. *Oncotarget* **8**, 95223–95246 (2017).
232. Fiorio Pla, A. & Munaron, L. Functional properties of ion channels and transporters in tumour vascularization. *Philos. Trans. R. Soc. B Biol. Sci.* **369**, (2014).
233. Adapala, R. K. *et al.* Activation of mechanosensitive ion channel TRPV4 normalizes tumor vasculature and improves cancer therapy. *Oncogene* **35**, 314–322 (2016).
234. Fiorio Pla, A. *et al.* TRPV4 mediates tumor-derived endothelial cell migration via arachidonic acid-activated actin remodeling. *Oncogene* **31**, 200–212 (2012).
235. Pla, A. F. *et al.* Arachidonic Acid–Induced Ca 2+ Entry Is Involved in Early Steps of Tumor Angiogenesis. *Mol. Cancer Res.* **6**, 535–545 (2008).
236. Fiorio Pla, A. *et al.* Multiple Roles of Protein Kinase A in Arachidonic Acid–Mediated Ca 2+ Entry and Tumor-Derived Human Endothelial Cell Migration. *Mol. Cancer Res.* **8**, 1466–1476 (2010).
237. Li, J. *et al.* Orai1 and CRAC channel dependence of VEGF-activated Ca2+ entry

and endothelial tube formation. *Circ. Res.* **108**, 1190–8 (2011).
238. Liu, X. *et al.* Hypoxia-induced upregulation of Orai1 drives colon cancer invasiveness and angiogenesis. *Eur. J. Pharmacol.* **832**, 1–10 (2018).
239. Yang, H. *et al.* Piezo2 protein: A novel regulator of tumor angiogenesis and hyperpermeability. *Oncotarget* **7**, 44630–44643 (2016).
240. Bianco, S., Mancardi, D., Merlino, A., Bussolati, B. & Munaron, L. Hypoxia and hydrogen sulfide differentially affect normal and tumor-derived vascular endothelium. *Redox Biol.* **12**, 499–504 (2017).
241. Pla, A. F. *et al.* Differential sensitivity of prostate tumor derived endothelial cells to sorafenib and sunitinib. *BMC Cancer* **14**, 939 (2014).
242. Scarpellino, G. *et al.* Purinergic Calcium Signals in Tumor-Derived Endothelium. *Cancers (Basel).* **11**, 766 (2019).
243. Genova, T. *et al.* TRPM8 inhibits endothelial cell migration via a non-channel function by trapping the small GTPase Rap1. *J. Cell Biol.* **216**, 2107–2130 (2017).
244. Li, F., Abuarab, N. & Sivaprasadarao, A. Reciprocal regulation of actin cytoskeleton remodelling and cell migration by Ca 2+ and

Zn 2+ : role of TRPM2 channels. *J. Cell Sci.* **129**, 2016–2029 (2016).

245. Lymburner, S., McLeod, S., Purtzki, M., Roskelley, C. & Xu, Z. Zinc inhibits magnesium-dependent migration of human breast cancer MDA-MB-231 cells on fibronectin. *J. Nutr. Biochem.* **24**, 1034–1040 (2013).

246. Park, K.-S. *et al.* Extracellular zinc stimulates ERK-dependent activation of p21(Cip/WAF1) and inhibits proliferation of colorectal cancer cells. *Br. J. Pharmacol.* **137**, 597–607 (2002).

Acknowledgments

I would like to thank all the people who have accompanied me in these three years, during the amazing experience to be a Ph.D. Student.

First, thank you to the entire Cellular and Molecular Angiogenesis Laboratory. My deepest gratitude goes to my supervisor, Prof. Luca Munaron, who gave me the opportunity to carry on this project, giving me great confidence and constant motivations. I would also like to thank Prof. Alessandra Fiorio Pla for her numerous teachings and for being a reference point for me and for the Lab. Thank you to Dr. Alessandra Gilardino, for her deep dedication to the Lab and her constant helpfulness towards people. Thank you to all my colleagues: Tullio, who shared with me his knowledge and his precious suggestions for life and science from the very first moment, Marianna and Federico, for being a special part of this journey despite the distance, and Giorgia, my best partner in this adventure.

Finally, I would like to thank all my family and friends starting from my Parents, who allowed me to achieve this goal, always supporting my every choice. Thank you to my Aunty, because I know she would be proud of me. Thank you to my Granny, for always appreciate and encourage me so much. Thank you to my special friends Gabriella and Claudia for the true friendship you show me every day. Last, but certainly not least, thank you Lorenzo for always being by my side in every single moment of my life, I am so lucky.

Thank you!